University of Arkansas, Fayetteville

ScholarWorks@UARK

Theses and Dissertations

7-2020

Models for Data Analysis in Accelerated Reliability Growth

Cesar Alexander Ruiz Torres
University of Arkansas, Fayetteville

Follow this and additional works at: https://scholarworks.uark.edu/etd

Part of the Industrial Engineering Commons, Industrial Technology Commons, Operational Research Commons, and the Statistical Methodology Commons

Citation

Ruiz Torres, C. A. (2020). Models for Data Analysis in Accelerated Reliability Growth. *Theses and Dissertations* Retrieved from https://scholarworks.uark.edu/etd/3769

This Dissertation is brought to you for free and open access by ScholarWorks@UARK. It has been accepted for inclusion in Theses and Dissertations by an authorized administrator of ScholarWorks@UARK. For more information, please contact ccmiddle@uark.edu.

Models for Data Analysis in Accelerated Reliability Growth

A dissertation submitted in partial fulfillment
of the requirements for the degree of
Doctor of Philosophy in Engineering, with a concentration in Industrial Engineering

by

Cesar Ruiz
Escuela Superior de Economía y Negocios
Bachelor of Arts in Business Engineering, 2014
University of Arkansas
Master of Science in Industrial Engineering, 2018

July 2020
University of Arkansas

This dissertation is approved for recommendation to the Graduate Council.

Edward A. Pohl, Ph.D.
Dissertation Director

Haitao Liao, Ph.D.
Committee Member

Kelly M. Sullivan, Ph.D.
Committee Member

Raymond Hill, Ph.D.
Committee Member

Abstract

This work develops new methodologies for analyzing accelerated testing data in the context of a reliability growth program for a complex multi-component system. Each component has multiple failure modes and the growth program consists of multiple test-fix stages with corrective actions applied at the end of each stage. The first group of methods considers time-to-failure data and test covariates for predicting the final reliability of the system. The time-to-failure of each failure mode is assumed to follow a Weibull distribution with rate parameter proportional to an acceleration factor. Acceleration factors are specific to each failure mode and test covariates. We develop a Bayesian methodology to analyze the data by assigning a prior distribution to each model parameter, developing a sequential Metropolis-Hastings procedure to sample the posterior distribution of the model parameters, and deriving closed form expressions to aggregate component reliability information to assess the reliability of the system. The second group of methods considers degradation data for predicting the final reliability of a system. First, we provide a non-parametric methodology for a single degradation process. The methodology utilizes functional data analysis to predict the mean time-to-degradation function and Gaussian processes to capture unit-specific deviations from the mean function. Second, we develop parametric model for a component with multiple dependent monotone degradation processes. The model considers random effects on the degradation parameters and a parametric life-stress relationship. The assumptions are that degradation increments follow an Inverse Gaussian process and a Copula function captures the dependency between them. We develop a Bayesian and a maximum likelihood procedure for estimating the model parameters using a two-stage process: (1) estimate the parameters of the degradation processes as if they were independent and (2) estimate the parameters of the Copula function using the estimated cumulative distribution function of the observed degradation increments as observed data. Simulation studies show the efficacy of the proposed methodologies for analyzing multi-stage reliability growth data.

Acknowledgments

First, I am deeply grateful to my advisor Dr. Ed Pohl for giving me the opportunity to do my doctoral studies in the University of Arkansas, for his continuous support and advise on my studies and research, for given me the opportunity to attend more conference that most students, for taking the time in his busy schedule as the Department Head to regularly meet me and help me improve my papers. I am also extremely grateful to my dissertation committee members, Dr. Haitao Liao, Dr. Kelly Sullivan, and Dr. Ray Hill for their guidance and support through my journey at the University of Arkansas since my first day in the department. I would like to thank Dr. Manuel Rossetti and Dr. Ashlea Milburn for their counsel when I worked for them as Teaching Assistant.

Second, I am grateful for all that inspired me to take this journey. I cannot thank my parents enough for their support of my endeavors. Even though they did not have the opportunities to study more than middle school, they dedicated their lives for me and my brother so that we can have a better life, follow our dreams, and made me understand the value of an education. I am also grateful for all the mentors that I had during my undergraduate studies who believed in me, inspired me to pursue my doctoral studies, and guided me to be as prepared as possible for my graduate studies.

Third, I would like to thank all the staff in the Industrial Engineering department for their patience in dealing with all my questions through the years, for helping me to coordinate with my advisor, for taking care of all our travel arrangements, and helping us organize our student events.

Contents

1 Introduction **1**

References **3**

2 A Bayesian Framework for Accelerated Reliability Growth Testing with Multiple Sources of Uncertainty **4**

2.1 Introduction 4

2.2 Basic Accelerated Reliability Growth Model 6

2.2.1 Bayesian Accelerated Reliability Growth at Component Level 8

2.2.2 Information Aggregation at System Level 9

2.3 Fully Bayesian Model 10

2.4 Numerical Example 14

2.4.1 System Description 14

2.4.2 Results at Component Level 16

2.4.3 Results at System Level 20

2.4.4 Case with Known Shape Parameters 23

2.4.5 Case with Known Acceleration Factors and Shape Parameters 25

2.5 Alternative Approaches 25

2.5.1 Alternative Approach for Prior Information on the Lifetime Distribution . . 26

2.5.2 Estimation of Acceleration Factors 29

2.6 Conclusions 30

References **31**

3 A Non-parametric Degradation-based Method for Modeling Reliability Growth **33**

3.1 Introduction 33

3.2 Degradation-based Reliability Growth 35

3.3 Non-parametric Degradation Modeling 36

3.4 Numerical Example 39
3.4.1 Degradation Characteristics and Data Generation Process 39
3.4.2 Results 40
3.5 Conclusions 44

References 45

4 Analysis of Correlated Multivariate Degradation Data in Accelerated Reliability Growth 46
4.1 Introduction 46
4.2 Dependent Degradation Processes Model 51
4.2.1 Degradation Modeling 51
4.2.2 Explanatory Variables 52
4.2.3 Random Effects 53
4.2.4 Reliability Growth Program 55
4.3 Parameter Estimation 56
4.3.1 MLE Procedure 57
4.3.2 Bayesian Procedure 59
4.3.3 Copula Selection 60
4.4 Numerical Example 61
4.4.1 System Description 62
4.4.2 Reliability Prediction 63
4.4.3 Performance with Multiple Replications 65
4.5 Conclusions 69

References 70

5 Summary 77

List of Figures

2.1 System tested during experiments . . . 15

2.2 Relative error of reliability estimate under different proposal distributions and biased priors for component A as the total testing time increases. . . . 17

2.3 Relative error of the parameter estimates using Exponential proposal and unbiased prior as the total testing time increases. . . . 19

2.4 Relative error and variance of the estimate of the reliability for component A with all parameters unknown as the total testing time increases. . . . 20

2.5 Relative error and variance of the estimate of the reliability for the system with all parameters unknown as the total testing time increases. . . . 22

2.6 Relative error and variance of the estimate of the reliability for the system with all parameters unknown as the total testing time increases with greater acceleration factor. . . . 22

2.7 Relative error and variance of the estimate of the reliability for component A with known shape parameter (b) as the total testing time increases. . . . 24

2.8 Relative error and variance of the estimate of the reliability for the system with known shape parameter (b) as the total testing time increases. . . . 24

2.9 Relative error and variance of the estimate of the reliability for component A with known shape parameter and acceleration factors as the total testing time increases. . . 26

2.10 Relative error and variance of the estimate of the reliability for the system with known shape parameter and acceleration factors as the total testing time increases. . . 27

2.11 Relative error of the reliability estimate for component A under discretized shape parameter as the total testing time increases. . . . 29

3.1 Observed degradation for units tested during a reliability growth program. . . . 35

3.2 Time to observe a degradation level. . . . 36

3.3 Mean time to degradation function with 50 measurements. . . . 41

3.4 Mean time to degradation function with 25 measurements. . . . 41

3.5 Mean time to degradation function with 50 measurements. . . . 42

3.6 Reliability function with relatively low variance. . . . 43

3.7 Reliability function with relatively high variance. 43

3.8 Box plot of the error on the final reliability estimate at 1390 and 1400 hours for 100 replications of the growth program. 44

4.1 Example of degradation signals with different failure thresholds. 48

4.2 Pairs of random variables under different copula functions. 61

4.3 Estimated reliability curves when 3 units are tested for 100 hours in each condition and the true model presents random effects on both parameters. 64

4.4 Estimated reliability functions with different true models. 64

4.5 Estimated reliability curves when either the number of measurements or the number of units increases. 65

4.6 Relative error of the mean inverse-degradation (ν) estimate. 66

4.7 Relative error of the MTTF estimate. 67

4.8 Relative error of the corrected mean inverse-degradation (νd_{ν_s}) estimate. 68

4.9 Relative error of the copula parameter estimate. 69

List of Tables

2.1 Comparision of the parametrization of the Weibull distribution. 7

2.2 Component characterisitcs 15

2.3 Component characteristics 16

2.4 Pmf for the shape parameter b_j. 28

3.1 Parameters used on the experiments 40

4.1 Parameters of each degradation process when there are radom effects on (m_{0i}, λ_i). 62

4.2 Characteristics of the sequential MH procedure. 63

4.3 Probability of selecting the right copula function. 68

List of Published Papers

Ruiz, C., Pohl, E. A., Liao, H., and Sullivan, K. M., "A Bayesian Framework for Accelerated Reliability Growth Testing with Multiple Sources of Uncertainty", *Quality, Reliability and Engineering International*, Vol. 35, No. 3, pp. 837-853, 2019. [**Published**][**Chapter Two**]

Ruiz, C., Liao, H., and Pohl, E. A., "A Nonparametric Degradation-Based Method for Modeling Reliability Growth", Proceedings of the 65th Annual Reliability and Maintainability Symposium, Orlando, FL, January 28-31, 2019. [**Published**][**Chapter Three**]

Ruiz, C., Liao, H., and Pohl, E. A., "Analysis of Correlated Multivariate Degradation Signals for Accelerated Reliability Growth", *Quality and Reliability Engineering International*, 2020. [**Under review**][**Chapter Four**]

1 Introduction

Reliability is the probability that a system will be capable of performing the task that it was designed for after a period of time while working under its intended condition and maintenance operations. A reliability growth program is the process of changing the system design based on test results in order to improve the overall reliability of the system. Reliability growth programs are important tools for the industry and the government to ensure that new systems will achieve minimum reliability standards in the short period of time available for development. A common practice ot speed up the data collection process is to test the system at harsher than normal use condition (i.e., accelerated testing). Due to the increasing complexity of modern engineering systems, it is not economically viable to test at system level and the reliability growth analysis must be done based on reliability testing at subsystem and component level. There are three primary types of data available from reliability testing: pass-fail, time-to-failure, and degradation of performance or physical characteristics (Wilson & Fronczyk, 2017). In the reliability growth literature, models based on pass-fail and time-to-failure data have received considerable attention (Martz & Waller, 1991; Crow, 2004; Wayne & Modarres, 2015). However, such models only consider the reliability growth of single component systems or series systems and often struggle to accurately incorporate accelerated test data in the analysis. This dissertation considers the problem of analyzing accelerated test data to predict the final reliability of a complex multi-component system undergoing a reliability growth program. The general assumptions through this work are: (1) the reliability growth program consists of multiple test-fix stages with corrective actions at the end of each stage, (2) the complex system consists of multiple components each with multiple failure modes, (3) testing is done at component level, (4) the system's structure is known, and (5) interactions between components do not introduce new failure modes. Under this framework, we develop new methodologies for analyzing time-to-failure data for components with multiple failure modes and we propose the first methodologies, to the best of our knowledge, for analyzing degradation data during a reliability growth program.

First, time-to-failure is the most common type of data used by reliability growth models. Those models are typically utilized for planning, tracking, and projecting reliability based on testing time. In particular, the Crow-AMSAA model is commonly used in industry and the government (Crow, 2004). One of the key assumptions of this model is that the system failure intensity is a linear combination of the failure intensity of multiple failure modes. However, it does not account for the different effect of accelerated testing on each failure mode. To address this research gap, Chapter 2 is dedicated to the case when test covariates information and time-to-failure data are available. The main assumption is that the time-to-failure follows a Weibull distribution with rate parameter proportional to an acceleration factor specific to each failure mode and test covariates. We propose a Bayesian framework to incorporate prior information on the model parameters, develop a sequential Metropolis-Hasting algorithm to sample the posterior parameters, and discuss a procedure to aggregate component results to predict the system's reliability. The accuracy of the reliability predictions of the proposed model and the Crow-AMSAA model are compared with a numerical example using simulated data. Additionally, we present special cases of the model when some of the parameters are known.

Second, degradation data has become increasingly available in the last decades due to technological advancements that have made possible monitoring the status of a system or component through the usage of one or multiple degradation signals. Such information has the potential to improve the precision and accuracy of reliability estimates (Hamada, 2005) since degradation is often correlated with the underlying failure mechanism. This work considers components with multiple degradation processes that are considered failed when at least one of its degradation signals surpasses a known threshold specific to each process. Chapter 3 is dedicated to use a non-parametric methodology for analyzing degradation data. This methodology uses functional data analysis to estimate the mean time-to-degradation function and uses unit-specif Gaussian process to model deviations from the mean function. Corrections are incorporated as fix-value covariates on the mean function. The main drawback of this model is that requires all units to be tested until failure. In a similar direction, Chapter 4 is dedicated to develop a novel degradation-based reliability growth

model for a component with multiple dependent degradation processes. The main assumption of this model is that degradation processes are monotonic and that their increments follow an Inverse-Gaussian (IG) process. A copula function is used to model the dependencies between degradation increments. We incorporate covariates information by assuming that the inverse-mean degradation presents a log-linear relationship with normalized stress covariates. We develop multiple models by considering random effects on different degradation parameters (i.e., none, only on the inverse-mean parameter, or both the inverse-mean and diffusion parameter). We develop Bayesian and maximum likelihood procedures to estimate the model parameters in a two-step process. First, the parameters of the degradation processes are estimated by treating them as independent processes. Second, the estimated cumulative distribution function of the degradation increments are used as data to fit the parameters of the copula function. Numerical examples using simulated data are presented to validate the accuracy of the proposed methodologies.

References

Crow, L. H. (2004). An extended reliability growth model for managing and assessing corrective actions. In *2004 Proceedings Annual Reliability and Maintainability Symposium - RAMS*, (pp. 73–80).

Hamada, M. (2005). Using degradation data to assess reliability. *Quality Engineering*, *17*(4), 615–620.

Martz, H. & Waller, R. (1991). *Bayesian reliability analysis* (1 ed.). Krieger Publishing Company.

Wayne, M. & Modarres, M. (2015). A Bayesian model for complex system reliability growth under arbitrary corrective actions. *IEEE Transactions on Reliability*, *64*(1), 206–220.

Wilson, A. G. & Fronczyk, K. M. (2017). Bayesian reliability: Combining information. *Quality Engineering*, *29*(1), 119–129.

2 A Bayesian Framework for Accelerated Reliability Growth Testing with Multiple Sources of Uncertainty

Reliability growth tests are often used for achieving a target reliability for complex systems via multiple test-fix stages with limited testing resources. Such tests can be sped up via accelerated life testing (ALT) where test units are exposed to harsher-than-normal conditions. In this paper, a Bayesian framework is proposed to analyze ALT data in reliability growth. In particular, a complex system with components that have multiple competing failure modes is considered, and the time to failure of each failure mode is assumed to follow a Weibull distribution. We also assume that the accelerated condition has a fixed time scaling effect on each of the failure modes. In addition, a corrective action with fixed ineffectiveness can be performed at the end of each stage to reduce the occurrence of each failure mode. Under the Bayesian framework, a general model is developed to handle uncertainty on all model parameters, and several special cases with some parameters being known are also studied. A simulation study is conducted to assess the performance of the proposed models in estimating the final reliability of the system and to study the effects of unbiased and biased prior knowledge on the system-level reliability estimates.

2.1 Introduction

Increasingly fast technology advancements and competitive markets have forced decision makers to develop products in a shorter time period and with less testing resources while meeting high reliability expectations. Reliability growth is one of the most popular techniques used to achieve these goals. This technique requires testing an early version of a product, identifying the most important failure modes, and performing corrections to reduce the chances of failure (Crow, 2004a). To quickly surface the failure modes of interest, tests can be sped up by using accelerated life testing (ALT) where test units are exposed to harsher-than-normal conditions (Elsayed, 2012). In addition, Bayesian statistical models can be used to improve reliability estimation by incorporating experts' opinions and experience with similar products (Martz & Waller, 1991). The technique reduces the

required amount of testing in a reliability growth program.

Among the available reliability growth models, the Crow-AMSAA model is the most widely used in industry and government for the analysis of reliability growth testing data (Crow, 2004a). This model assumes that the occurrence of failures follows a non-homogeneous Poisson process during testing with corrections being implemented after the first observation of each failure mode or upon the completion of tests. Feinberg (1994) provided closed-form equations to incorporate ALT with the Crow-AMSAA model by using a constant time scaling factor that captures the equivalence between the testing times under the normal and harsher-than-normal conditions. Feinberg's ALT-extended Crow-AMSAA model has been applied in industry for relatively simple electronic components (Acevedo et al., 2006). Although constant time-scaling is mathematically convenient, concerns about its practicality motivate the development of various parametric and non-parametric acceleration models for determining equivalence between the results from ALT and the normal use condition. A summary of these models can be found in Nelson (1990); Meeker & Escobar (1998); Elsayed (2012). Furthermore, Freels et al. (2015) study the capacity of commonly used data analysis techniques to produce meaningful reliability estimates based on highly accelerated life test results.

Although a classical statistical approach may be applied under a reliability growth program as discussed previously, complications arise when few or no failures are observed during testing. This issue has attracted much attention of both researchers and practitioners. For example, Jiang et al. (2010) develop a modified maximum likelihood estimate for the Weibull distribution parameters with zero failures. Moreover, the use of Bayesian statistics offers a useful alternative for solving these problems by incorporating prior information into reliability estimation. Martz & Waller (1991) present an overview of classical Bayesian models while Hamada et al. (2008) present a modern perspective of Bayesian models for component and system reliability analysis. Moreover, ALT has been considered in conjunction with Bayesian reliability models. As an example, Somerville et al. (1997) model the conditional reliability of a component after a series of step-stress tests in a random order using a Dirichlet prior distribution. Yuan et al. (2014) model reliability under use condition

using a Dirichlet process with Weibull kernels to incorporate ALT data.

In the area of reliability growth, Bayesian reliability models have also been investigated. The first of such models, to the best of our knowledge, is by Pollock (1968) which makes inferences on reliability improvement by detecting if failure mechanisms have been completely eliminated or if they are still present after a correction. More recently, Wayne & Modarres (2015) develop a model to estimate the reliability of a multi-component system with a complex structure, such as motorized vehicles, by assuming that the failure modes are independent, serial in nature, and have exponential life-time distributions. Corrections are incorporated in this model as a fixed-effect reduction in the failure rate of each failure mode. In this setting, it is possible to calculate the moments of system reliability using the moments of component reliability via block decomposition for Bayesian (Martz & Waller, 1990) and traditional (Jin & Coit, 2008) statistical approaches. Thompson & Haynes (1980) provide a Beta distribution to approximate the system reliability distribution using the method of moments. Using ALT data, Strunz & Herrmann (2012) develop a model for Bayesian reliability growth analysis for a one-shot system such as a projectile weapon. Ruiz et al. (2018) develop a model to estimate the reliability of a complex system using block decomposition on an ALT-based reliability growth program implemented for the components.

In this paper, we develop a general Bayesian accelerated reliability growth (GBARG) framework to incorporate all sources of information to draw inferences for the reliability of a complex system whose components present multiple independent failure modes. The remainder of this paper is organized as follows. Section 2.2 presents a previous work on the simplest case of Bayesian accelerated reliability growth (BARG). Section 2.3 develops a general framework for BARG by considering uncertainty in all model parameters. Section 2.4 illustrates the performance of the framework using a numerical example. Lastly, Section 2.6 draws conclusions.

2.2 Basic Accelerated Reliability Growth Model

We consider a multi-component system with a known structure, where its function can be described by a reliability block diagram. Each component i has n_i identifiable independent failure modes of

interest, which are elicited from system experts using reliability engineering analysis techniques. Similar to Crow (2004b), one failure mode can be defined to include all failure modes not relevant to the reliability growth program as corrections will not be applied to them and such failure modes may or may not be completely identifiable. The failure time of each failure mode $j = 1, \cdots, n_i$ of component i is assumed to follow a Weibull distribution with probability density function (pdf):

$$f_{ij}(t) = \lambda_{ij} b_{ij} t^{b_{ij}-1} \exp\left(-\lambda_{ij} t^{b_{ij}}\right) \tag{2.1}$$

where λ_{ij} is the rate parameter, and b_{ij} is the shape parameter. Note that this parametrization is used for convenience in the Bayesian analysis of the data. The equivalence between this parameterization and the commonly used one with shape b_{ij} and scale parameter $\eta_{ij} = \lambda^{-1/b_{ij}}$ is shown in Table 2.1.

Table 2.1: Comparision of the parametrization of the Weibull distribution.

Parametrization	Parameters	pdf	Reliability
Weibull-Rate	(b, λ)	$\lambda b t^{b-1} \exp(-\lambda t^b)$	$\exp(-\lambda t^b)$
Weibull-Scale	(b, η)	$\frac{b}{\eta}\left[\frac{t}{\eta}\right]^{b-1} \exp\left(-\left[\frac{t}{\eta}\right]^b\right)$	$\exp\left(-\left[\frac{t}{\eta}\right]^b\right)$

The reliability growth program consists of S testing stages with corrective actions at the end of each stage. There are κ different testing environments including the use condition. In each stage s, W_s identical copies of a component are tested each under a particular testing condition that increases the rate parameter by a factor of $a_{ijws} = \sum_{k=1}^{\kappa} \rho_{kws} a_{ijk}$ for unit w and failure mode j of component i, where ρ_{kws} equals 1 if unit w in stage s is tested using environment k (and 0 otherwise). Lastly, corrections decrease the rate parameter λ_{ij} by an effectiveness factor of $1 - d_{ijs}$ such that the final rate parameter is $\lambda_{ij} \prod_{s=1}^{S} d_{ijs}$. Note that parameter d_{ijs} is the ineffectiveness of corrections in order to simplify the notation throughout the paper. This model has the following sources of uncertainty for each component:

- Parameters of life-time distribution (λ_{ij}, b_{ij}), for $j = 1, \cdots, n_i$.
- Acceleration factors (a_{ijk}), for $k = 1, \cdots, \kappa$.

- Ineffectiveness of each corrective action (d_{ijs}), for $s = 1, \cdots, S$.

First, we calculate the final reliability of a component after a growth program has been carried out under specific conditions. Second, we aggregate the results for all components to estimate the final system reliability based on the system structure.

2.2.1 Bayesian Accelerated Reliability Growth at Component Level

We consider the Bayesian Reliability Growth Model (BARG) developed by Ruiz et al. (2018) to estimate the final reliability of a component, where only the rate parameter is unknown, and use a short notation to identify failure modes using only one index (i.e., j instead of ij). We assume that all other parameters can be accurately estimated and typically will have $a_{jk} \geq 1$ and $0 < d_{js} < 1$. Thus, the only source of uncertainty is on λ_j for which a Gamma prior distribution is assumed with pdf:

$$\pi(\lambda_j) = \frac{\beta_j^{\alpha_j}}{\Gamma(\alpha_j)} \lambda_j^{\alpha_j - 1} \exp\left(-\lambda_j \beta_j\right). \tag{2.2}$$

Using Bayes' theorem, the posterior distribution π' of λ_j given the observed information on failure time, failure mode, and testing environment $D = \{\boldsymbol{t}, \boldsymbol{\delta}, \boldsymbol{\rho}\}$ can be expressed as:

$$\pi'(\lambda_j) = \frac{\mathcal{L}(D, \lambda_j)\pi(\lambda_j)}{\int_0^\infty \mathcal{L}(D, \lambda_j)\pi(\lambda_j) d\lambda_j}.$$

Given the choice of prior, the hyperparameters of the posterior (also Gamma) after each test-fix stage are:

$$\begin{aligned}
\alpha_{js} &= \alpha_{js-1} + \sum_{w=1}^{W_s} \delta_{jws} && \forall\, (j, s), \\
\beta_{js} &= \frac{\beta_{js-1}}{d_{js}} + \frac{1}{d_{js}} \sum_{w=1}^{W_s} t_{ws}^{b_j} a_{jws} && \forall\, (j, s),
\end{aligned}$$

where δ_{jws} equals 1 if failure mode j was observed in unit w in stage s (and 0 otherwise), and t_{sw} is the testing time for unit w in stage s. Because a failure of unit w ends its testing withing a given stage, t_{sw} provides either a censoring time (if unit w does not fail) or a failure time (if unit w fails).

Lastly, the moments of the reliability of a component after the sth stage for a fixed target life time T can be expressed as:

$$E[R_s^m] = \prod_{j=1}^{n_i} \left(\frac{\beta_{js}}{\beta_{js} + mT^{b_j}} \right)^{\alpha_{js}} . \tag{2.3}$$

2.2.2 Information Aggregation at System Level

We use the block decomposition technique (Martz & Waller, 1990) to estimate the moments of the reliability of a complex system using the moments of component reliability. Block decomposition consists of grouping components in blocks such that an equivalent system in terms of its blocks is formed with a pure series or parallel structure. This process is repeated using each block as a new system until there is only one component in each block.

We identify each block by a vector (B, k) where k is the block level and B is the block number at level k, where level 0 is the system, 1 is a collection of blocks that form the system and so on up to the component level. Define $\Omega_{B,k}$ as the set of blocks that form block B at level k. The moments of the reliability can be respectively evaluated for a series or parallel block (B, k) as (Ruiz et al., 2018):

$$E[R_{B,k}^m] = \prod_{B' \in \Omega_{B,k}} E\left[R_{B',k+1}^m\right] , \qquad \text{(Series)} \tag{2.4}$$

$$E[R_{B,k}^m] = 1 + \sum_{i=1}^{m} (-1)^i \binom{m}{i} \prod_{B' \in \Omega_{B,k}} \left(1 + \sum_{j=1}^{in_{B'}} (-1)^j \binom{in_{B'}}{j} E[R_{B',k+1}^j] \right) , \qquad \text{(Parallel)} \tag{2.5}$$

where $n_{B'}$ is the number of redundant identical copies of block B' in block (B, k).

2.3 Fully Bayesian Model

The BARG model given in the previous section provides the system reliability moments of the simplest case where only λ is uncertain. In this section, we develop a general BARG (GBARG) model to consider the uncertainty of all model parameters. Consistent with Section 2.2.1, we use a short notation to refer to failure modes only by index j instead of ij. Define Θ_j as the set of all model parameters related to failure mode j, i.e., $\Theta_j = \{\lambda_j, b_j, \boldsymbol{a_j}, \boldsymbol{d_j}\}$. It is worth pointing out that Θ_j is independent of all other model parameters due to the assumption about independent failure modes. Given the observed information D (as defined in Section 2) after S test-fix stages the likelihood function can be expressed as:

$$\begin{aligned}
\mathcal{L}(\Theta_j|D) &= \prod_{s=1}^{S}\prod_{w=1}^{W_s}\left[a_{jws}\left(\prod_{s'=1}^{s-1} d_{js'}\right)\lambda_j b_j t_{ws}^{b_j-1}\right]^{\delta_{jws}} \exp\left[-a_{jws}\left(\prod_{s'=1}^{s-1} d_{js'}\right)\lambda_j t_{ws}^{b_j}\right], \\
&= \prod_{s=1}^{S}\left[\left(\lambda_j b_j \prod_{s'=1}^{s-1} d_{js'}\right)^{\sum_{w=1}^{W_s}\delta_{jws}} \prod_{w=1}^{W_s} a_{jws}^{\delta_{jws}} t_{ws}^{\delta_{jws}(b_j-1)}\right] \times \\
&\quad \exp\left[-\lambda_j \sum_{s=1}^{S}\sum_{w=1}^{W} a_{jws}\left(\prod_{s'=1}^{s-1} d_{js'}\right) t_{ws}^{b_j}\right],
\end{aligned} \tag{2.6}$$

where δ_{jws} is defined in Section 2.2. Note that $\mathcal{L}(\Theta_j|\boldsymbol{t})$ does not incorporate the information on d_{jS} since the components are not tested after this corrective action has been applied. In addition, we assume that $P\{d_{js} = 1\} = 1$ for cases where corrections have no effect on failure mode j resulting in no reduction in λ_j, and for $s = 1$, $\prod_{s'=1}^{s-1} d_{js'} = 1$.

Since no joint conjugate prior distribution is available for all the parameters in Θ_j, we develop a Metropolis-Hasting (MH) procedure to sample the posterior distributions of the parameters. Specifically, we develop a sequential MH procedure to sample from the conditional distribution of one parameter at a time given the current sample of all other parameters. The conditional likelihoods of parameters $\theta_j \in \Theta_j$ given the fixed values of all other parameters (represented as a set difference

$\Theta_j \setminus \theta_j$) up to a multiplicative constant required for the procedure are:

$$\mathcal{L}(\lambda_j|\Theta_j \setminus \lambda_j, D) \propto \lambda_j^{\sum_{s=1}^{S}\sum_{w=1}^{W_s}\delta_{jws}} \exp\left[-\lambda_j \sum_{s=1}^{S}\sum_{w=1}^{W_s} a_{jws}\left(\prod_{s'=1}^{s-1} d_{js'}\right) t_{ws}^{b_j}\right], \tag{2.7a}$$

$$\mathcal{L}(b_j|\Theta_j \setminus b_j, D) \propto b_j^{\sum_{s=1}^{S}\sum_{w=1}^{W_s}\delta_{jws}} \left[\prod_{s=1}^{S}\prod_{w=1}^{W_s} t_{ws}^{\delta_{jws}(b_j-1)}\right] \exp\left[-\sum_{s=1}^{S}\sum_{w=1}^{W_s} a_{jws}\left(\prod_{s'=1}^{s-1} d_{js'}\right)\lambda_j t_{ws}^{b_j}\right], \tag{2.7b}$$

$$\mathcal{L}(a_{jk}|\Theta_j \setminus a_{jk}, D) \propto a_{jk}^{\sum_{s=1}^{S}\sum_{w=1}^{W_s}\delta_{jws}\rho_{kws}} \exp\left[-a_{jk}\lambda_j \sum_{s=1}^{S}\sum_{w=1}^{W_s} \rho_{kws}\left(\prod_{s'=1}^{s-1} d_{js'}\right) t_{ws}^{b_j}\right], \tag{2.7c}$$

$$\mathcal{L}(d_{js}|\Theta_j \setminus d_{js}, D) \propto d_{js}^{\sum_{s'>s}^{S}\sum_{w=1}^{W_s}\delta_{jws'}} \exp\left[-d_{js}\lambda_j \sum_{s'>s}^{S}\sum_{w=1}^{W_s} a_{jws'}\left(\prod_{s"=1:s"\neq s}^{s'-1} d_{js''}\right) t_{ws'}^{b_j}\right], \tag{2.7d}$$

From the conditional likelihoods, we identify that λ_j, a_{jk}, and d_{js} have Gamma distributions as natural conjugate priors with the parametrization shown in Equation (2.2). Moreover, the posterior Gamma distribution can be used to evaluate how beneficial the corrective actions are and which testing environments accelerate the failure modes as intended. In contrast, b_j does not possess a natural conjugate prior distribution. Moreover, Singpurwalla (2011) identifies the difficulty in assessing λ directly from experts' knowledge and proposes to first elicit priors independently for b and t_{B50} (i.e., median lifetime) then derive the implicit distribution of λ instead of assuming that λ_j and b_j are independent. Using this strategy yields the following:

$$\begin{aligned}
t_{jB_{50}} &\sim \text{Inverse-Gamma}(\alpha_{jt}, \beta_{jt}) \\
a_{jk} &\sim \text{Gamma}(\alpha_{a_{jk}}, \beta_{a_{jk}}) \\
d_{js} &\sim \text{Gamma}(\alpha_{d_{js}}, \beta_{d_{js}}) \\
b_j &\sim \text{Three Parameter Gamma}(\gamma_j, \alpha_{b_j}, \beta_{b_j})
\end{aligned}$$

where γ_j is a shift parameter such that $b_j - \gamma_j \sim$ Gamma($\alpha_{b_j}, \beta_{b_j}$).

The conditional prior distribution of λ_j induced by the prior on $t_{jB_{50}}$ given b_j can be derived

as:

$$
\begin{aligned}
t_{jB_{50}} &= \left(\frac{\ln(2)}{\lambda_j}\right)^{1/b_j} && \text{(Definition)}, \\
J = \frac{dt_{jB_{50}}}{d\lambda_j} &= \frac{\ln(2)^{1/b_j}}{b_j\lambda_j^{1/b_j+1}} && \text{(Derivative)}, \\
\pi(\lambda_j|b_j) &= \pi(t^{-1}_{jB_{50}}(\lambda_j)|b_j)|J| && \text{(Change of variables)}, \\
&= \frac{\beta_{jt}^{\alpha_{jt}}}{\Gamma(\alpha_{jt})}\left(\frac{\lambda_j}{\ln(2)}\right)^{\dfrac{\alpha_{jt}+1}{b_j}} \exp\left(-\beta_{jt}\left[\frac{\lambda_j}{\ln(2)}\right]^{1/b_j}\right)\frac{\ln(2)^{1/b_j}}{b_j\lambda_j^{1/b_j+1}}, \\
&= \left(\frac{\beta_{jt}}{\ln(2)^{1/b_j}}\right)^{\alpha_{jt}} \Gamma\left(\alpha_{jt}\right)^{-1}\lambda_j^{\alpha_{jt}/b_j-1}\exp\left(-\frac{\beta_{jt}}{\ln(2)^{1/b_j}}\lambda_j^{1/b_j}\right)b_j^{-1}, && (2.8)
\end{aligned}
$$

where $\pi(\lambda_j|b_j)$ is not a known standard distribution. However, $\lambda_j^{b_j}$ follows a Gamma distribution with parameters $(\alpha_{jt}, \beta_{jt}\ln(2)^{-1/b_j})$.

Algorithm 1 MH Sequential Sampling Procedure

Require: N, Ω

1: Initialize parameters vectors $\boldsymbol{\lambda_j}, \boldsymbol{b_j}, \boldsymbol{a_{jk}}, \boldsymbol{d_{js}}$ of size N equal to $\mathbf{0}$.
2: Set $\lambda_{j1} = E_{\pi(t_{jB_{50}},b_j)}[\lambda_j],\ b_{j1} = 1 + \dfrac{\alpha_{b_j}}{\beta_{b_j}}$
3: Set $a_{jk1} = \dfrac{\alpha_{a_{jk}}}{\beta_{a_{jk}}}\ \forall k,\ d_{js1} = \dfrac{\alpha_{d_{js}}}{\beta_{d_{js}}}\ \forall s$
4: Set $c = 2$
5: **for** $c \leq N$ **do**
6: Sample:
7: $\lambda_{jc} =$ MHStep(λ_{jc-1})
8: $b_{jc} =$ MHStep(b_{jc-1})
9: $d_{jsc} \sim$ Gamma($\alpha'_{d_{js}}, \beta'_{d_{js}}$) $\forall s$
10: $a_{jkc} \sim$ Gamma($\alpha'_{a_{jk}}, \beta'_{a_{jk}}$) $\forall k$
11: $c = c + 1$
return $\boldsymbol{\lambda_j}, \boldsymbol{b_j}, \boldsymbol{a_{jk}}, \boldsymbol{d_{js}}$.

Algorithm 2 MH Step

Require: Proposal distribution $g(\cdot)$, prior distribution $\pi(\cdot)$, and initial value θ_c

1: Sample θ_p from $g(\theta|\theta_c)$ and u from Uniform$(0, 1)$
2: **if** $u \geq \dfrac{g(\theta_c|\theta_p)}{g(\theta_p|\theta_c)}\dfrac{\mathcal{L}(\theta_p|\Theta \notin \theta, \boldsymbol{t})\pi(\theta_p|\Omega_\theta)}{\mathcal{L}(\theta_c|\Theta \notin \theta, \boldsymbol{t})\pi(\theta_c|\Omega_\theta)}$ **then**
3: $\theta_p = \theta_c$
return θ_p

Algorithm 1 presents the sequential MH procedure used to sample the posterior distributions of the model parameters. The procedure requires the sample size N and the set of prior parameters Ω. Line 1 initializes the vectors. Lines $2-3$ set the initial sample to the expected value of their respective prior distributions. As a special case, the induced initial estimate for λ_j given the prior information on $t_{jB_{50}}$ and b_j is:

$$
\begin{aligned}
E[\lambda_j] &= \int_1^\infty \int_0^\infty \ln(2)\tau^{-b_j} \frac{\beta_{jt}^{\alpha_{jt}}}{\Gamma(\alpha_{jt})}\tau^{-\alpha_{jt}-1} \exp\left(-\frac{\beta_{jt}}{\tau}\right) \frac{\beta_{b_j}^{\alpha_{b_j}}}{\Gamma(\alpha_{b_j})}(b_j-\gamma_j)^{\alpha_{b_j}-1} \exp\left[-\beta_{b_j}(b_j-\gamma_j)\right] \mathrm{d}\tau \mathrm{d}b_j, \\
&= \ln(2)\frac{\beta_{b_j}^{\alpha_{b_j}}}{\Gamma(\alpha_{b_j})} \int_1^\infty \frac{\beta_{jt}^{\alpha_{jt}}}{\Gamma(\alpha_{jt})} \frac{\Gamma(\alpha_{jt}+b_j)}{\beta_{jt}^{\alpha_{jt}+b_j}} \frac{\beta_{b_j}^{\alpha_{b_j}}}{\Gamma(\alpha_{b_j})}(b_j-\gamma_j)^{\alpha_{b_j}-1} \exp\left[-\beta_{b_j}(b_j-\gamma_j)\right] \mathrm{d}b_j, \\
&= \ln(2)\frac{\beta_{b_j}^{\alpha_{b_j}}}{\Gamma(\alpha_{b_j})\Gamma(\alpha_{jt})} \int_1^\infty \frac{\Gamma(\alpha_{jt}+b_j)}{\beta_{jt}^{b_j}} \frac{\beta_{b_j}^{\alpha_{b_j}}}{\Gamma(\alpha_{b_j})}(b_j-\gamma_j)^{\alpha_{b_j}-1} \exp\left[-\beta_{b_j}(b_j-\gamma_j)\right] \mathrm{d}b_j, \quad (2.9)
\end{aligned}
$$

where the last integral is evaluated numerically. Lines $7-8$ sample the next value of each parameter, where the MH Step presented in Algorithm 2 is used to sample λ_j and b_j. On the other hand, a_{jk} and d_{js} can be sampled directly from a Gamma distribution with parameters of the form $(\alpha'_\theta = \alpha_\theta + A_\theta, \beta'_\theta = \beta_\theta + B_\theta)$ where $(\alpha_\theta, \beta_\theta)$ are the respective prior hyperparameters and (A_θ, B_θ) come from the likelihood function of the form $\theta^{A_\theta}\exp(-B_\theta\theta)$ as in Equations (2.7c) and (2.7d), respectively. Note that (A_θ, B_θ) are updated in each iteration of the algorithm depending on the current sample of all other parameters. A common practice to avoid the correlation among consecutive MH samples is to trim the sample vectors by only keeping one sample after a fixed number of them is drawn (i.e., thinning)(Van-Dorp & Mazzuchi, 2004).

Algorithm 2 presents the standard MH algorithm. It requires a proposal distribution $g(\cdot)$, prior distribution $\pi(\cdot)$, and current values of all parameters Θ with θ_c being the current value of the parameter of interest θ. Line 1 samples a proposed value θ_p from the proposal distribution given θ_c and a random number u. Line 2 assesses whether u is greater than or equal to the ratio of the proposal density θ_c given θ_p over the proposal density of θ_p given θ_c times the ratio of the posterior density of θ_p over the posterior density of θ_c. Note that this ratio allows us to use the likelihood up to a multiplicative constant to sample the posterior distribution. If u is greater than the ratio we

reject θ_p and change its value to θ_c in Line 3.

2.4 Numerical Example

In this section, we conduct a simulation study to assess the performances of the GBARG model to estimate the true reliability of a system based on the testing results of the components. We proceed to describe the system under test, then present the simulation results for the component and system levels.

2.4.1 System Description

Figure 2.1 shows the block diagram of the system used for this example. The overall system consists of two identical parallel subsystems with two identical subsystems E and E', each of which has a series-parallel structure, where subsystem C is formed by the identical components A and A', and subsystem D is formed by component B. Each component has two failure modes. The growth program is implemented by testing each component independently for an initial stage under the use condition, then conducting an accelerated test with a corrective action at the end, and performing a final accelerated test. Testing is performed such that identical copies of a component are tested one at a time. If the current copy fails, testing is continued with a new identical copy of the component until no more testing time is available. Details on the true parameters assumed for the growth program are provided in Table 2.2. Note that a direct comparison with traditional models such as the Crow-AMSAA is not possible under this reliability growth program since testing is done at a component level. Thus, most of the assumptions for the Crow-AMSAA model are violated such that it would perform poorly Wayne & Ellner (2010).

We simulate $M = 100$ replications of the growth program. After extensive numerical studies not presented here due to lack of space, we determine that the sample size required for the chain to converge is one million samples. We calculate the final system and component reliability values as indicated in Algorithm 1 by keeping one sample every one hundred observations (thinning) as done by Van-Dorp & Mazzuchi (2004). The expected values of the model parameters and reliability are

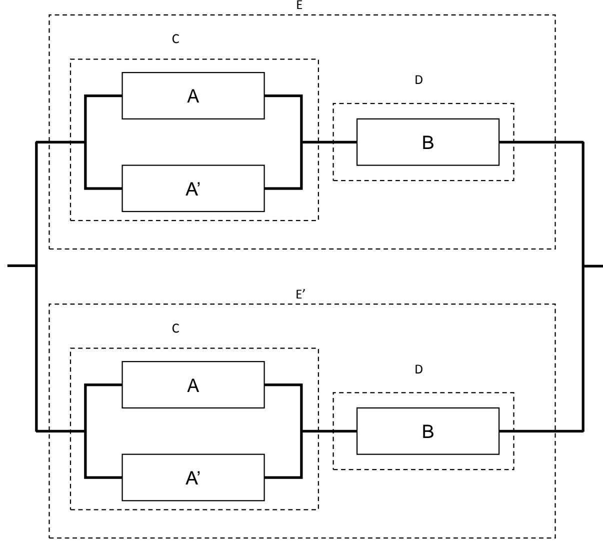

Figure 2.1: System tested during experiments

Table 2.2: Component characterisitcs

Component	Mode	$\lambda(10^{-5})$	b	d	a
A	1	2.383	1.52	0.77	7.50
	2	2.522	1.23	0.88	9.60
B	1	0.589	1.24	0.75	9.36
	2	0.652	1.33	0.80	12.15

used as the point estimates. The variance and expected value of the parameters at the end of each repetition are estimated as:

$$\hat{\theta}_m = \frac{\sum_{s=1}^{N} \theta_{ms}}{N}, \qquad \hat{R}_{im} = \frac{\sum_{s=1}^{N} R(\Theta_{ims})}{N},$$
$$\widehat{\text{Var}(\theta_m)} = \frac{\sum_{s=1}^{N} \theta_{ms}^2}{N-1} - \hat{\theta}_m^2, \qquad \widehat{\text{Var}(R_{im})} = \frac{\sum_{s=1}^{N} R(\Theta_{ims})^2}{N-1} - \hat{R}_{im}^2, \tag{2.10}$$

where θ_{ms} is the sth sample from the mth replication, $\Theta_i = U_{j=1}^{n_i}\Theta_j$, with Θ_j defined as in Section 2.3, and $R_{ijms}(\Theta_{ims}) = \exp(-\sum_{j=1}^{n_i} \lambda_{ijms} d_{ijms} T^{b_{ijms}})$ for a fixed target life time T. Moreover, the expected percentage relative error (RE) and variance of the point estimate considering the

simulation variance are calculated as:

$$\text{RE}(\hat{\theta}) = 100\frac{\sum_{m=1}^{M}\hat{\theta}_m}{M\theta} - 100, \qquad \text{Var}(\hat{\theta}) = \frac{\sum_{m=1}^{M}\text{Var}(\theta_m)}{M} + \frac{\sum_{m=1}^{M}(\hat{\theta}_m - \hat{\theta})^2}{M-1}. \tag{2.11}$$

Lastly, we conduct simulation experiments using multiple values of the parameters for the prior distribution such that the expected value of the reliability of the part with respect to R may show some bias compared to the true value of the parameter. Let c be a multiplier such that for the parameter θ the expected value $E[\theta]$ of its prior is either $c\theta$ or θ/c such that if $c > 1$ the expected value of the reliability of the part with respect to θ decreases. In this study, we set $c < 1$ for optimistic priors, $c = 1$ for unbiased priors, and $c > 1$ for pessimistic priors. Using this definition, we use the equations shown in Table 2.3 to calculate the hyperparameters of the prior where $b > 1.01$ with $\gamma = 1$ such that the components always age and $d > 1$ such that the corrections are expected to have no effect in the worst case.

Table 2.3: Component characteristics

Parameter	$E[\cdot]$	α	β
b	$\max(cb, 1.01)$	2	$\alpha/(E[b]-1)$
$t_{B_{50}}$	$c(\ln 2/\lambda)^{1/E[b]}$	2	$(\alpha-1)E[t_{B_{50}}]$
d	$\min(cd, 1)$	2	$\alpha/E[d]$
a	a/c	2	$1/E[a]$

2.4.2 Results at Component Level

First, we investigate the effect of the proposal distribution on the convergence of the method. We only consider those proposals with a positive support, such that it is not required to discard observations when a negative value is drawn. In particular, we compare an exponential distribution with mean λ_{jc-1} as a proposal for λ_j and a two-parameter exponential distribution with a shift of 1 and mean of b_{jc-1} as proposal for b_j with a log-normal distribution with the same mean as the exponential and variance of 1. Figure 2.2 presents a box plot for the reliability estimates of component A as testing time is increased for prior distributions of the parameters (pessimistic with $c = 2$ and

optimistic with $c = 0.5$) and different proposal distributions for the MH algorithm, with each replication observing the same test results such that only the prior and proposal parameters induce any observed difference in the reliability estimate. The columns are organized as pessimistic, unbiased, and optimistic for the exponential and log-normal proposal distributions. The results show significant discrepancies between the estimates produced using different proposals when bias (pessimistic and optimistic) is introduced to the prior distributions. In particular, the log-normal proposal results in more uncertain estimates due to the lack of convergence of the MH procedure (convergence plots for both distributions are not shown here due to space limitation). This suggests that the exponential proposal is more robust for this problem since the variation and bias of the point estimate of reliability is reduced as the testing time increases for all cases.

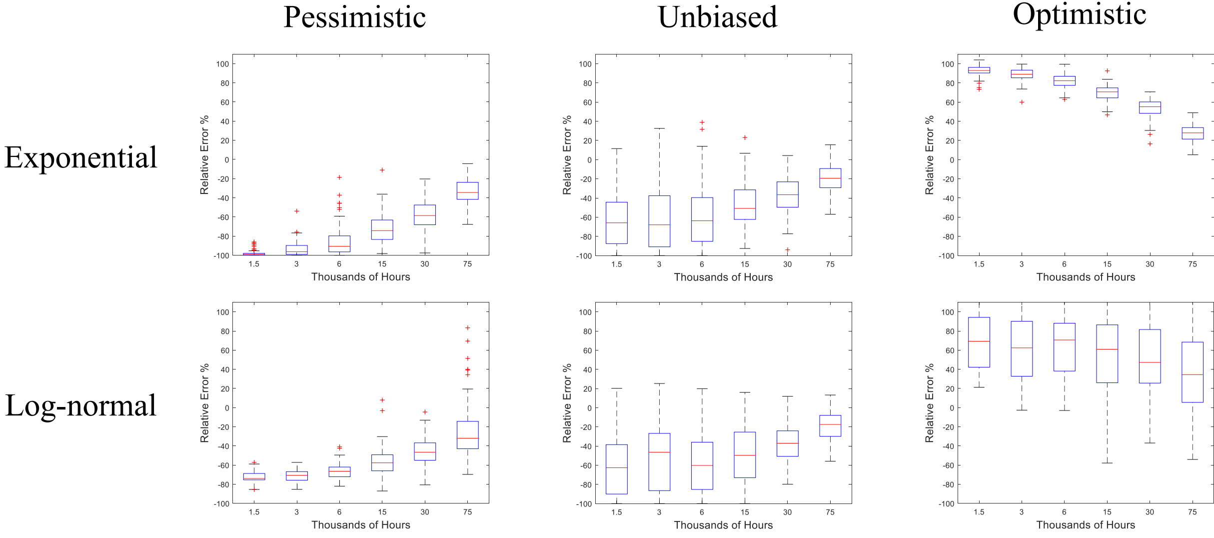

Figure 2.2: Relative error of reliability estimate under different proposal distributions and biased priors for component A as the total testing time increases.

Figure 2.3 presents a box plot of the point estimate of different model parameters under an unbiased prior and the Exponential proposal. One can see that λ is the hardest to estimate in terms of having the highest relative error due to underestimating b in both failure modes which causes the overestimation of λ. Furthermore, increasing the testing time effectively reduces the relative error for all parameters, and no bias is observed for d and a. However, the uncertainty on a as well as λ for the second failure mode increases as the testing time increases while the uncertainty on all other

model parameters decreases because the lack of observations on failure mode two relative to failure mode one, a being the last parameter to be sampled in Algorithm 1, and the relative high variance that its prior has as compared to the variance of the prior of other parameters (due to the magnitude of each parameter). This suggests that the shape and rate parameters are the most important sources of uncertainty in the model.

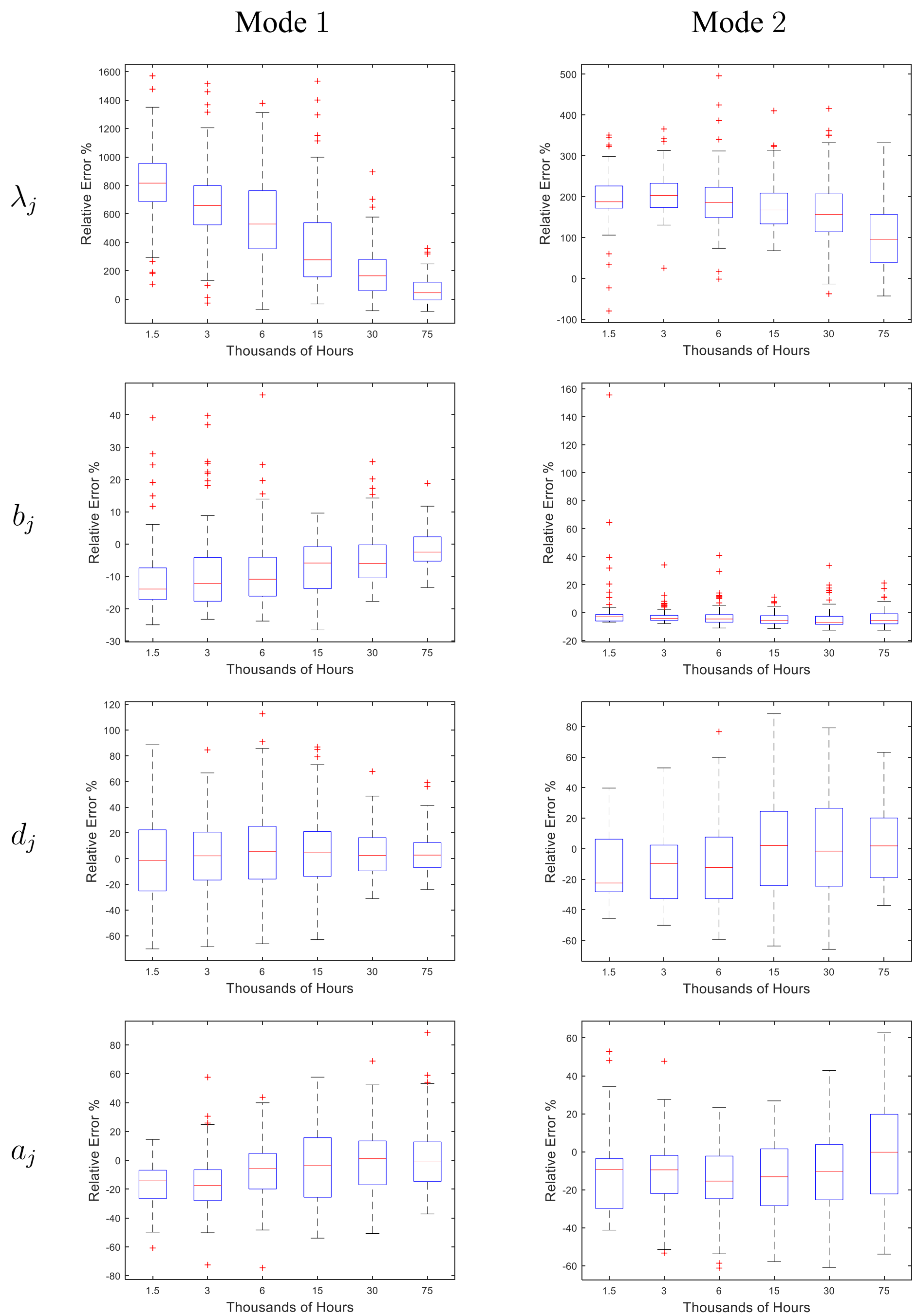

Figure 2.3: Relative error of the parameter estimates using Exponential proposal and unbiased prior as the total testing time increases.

Figure 2.4 shows the relative error and variance of the reliability estimate for component A after 100 replications of the growth program calculated using Equations in (2.11). For both, pessimistic and optimistic priors the magnitude of estimation bias is reduced as more testing time is available. A similar trend is observed for the variance of the estimate for all but the two extreme cases of optimistic and pessimistic priors. In particular, the two most optimistic priors have variances with an order of magnitude lower than all other cases due to not overcoming the prior information and having the same reliability point estimate in most replications, while the cases with the most pessimistic priors are more sensitive to the test results when the testing time is less than 6 thousand hours.

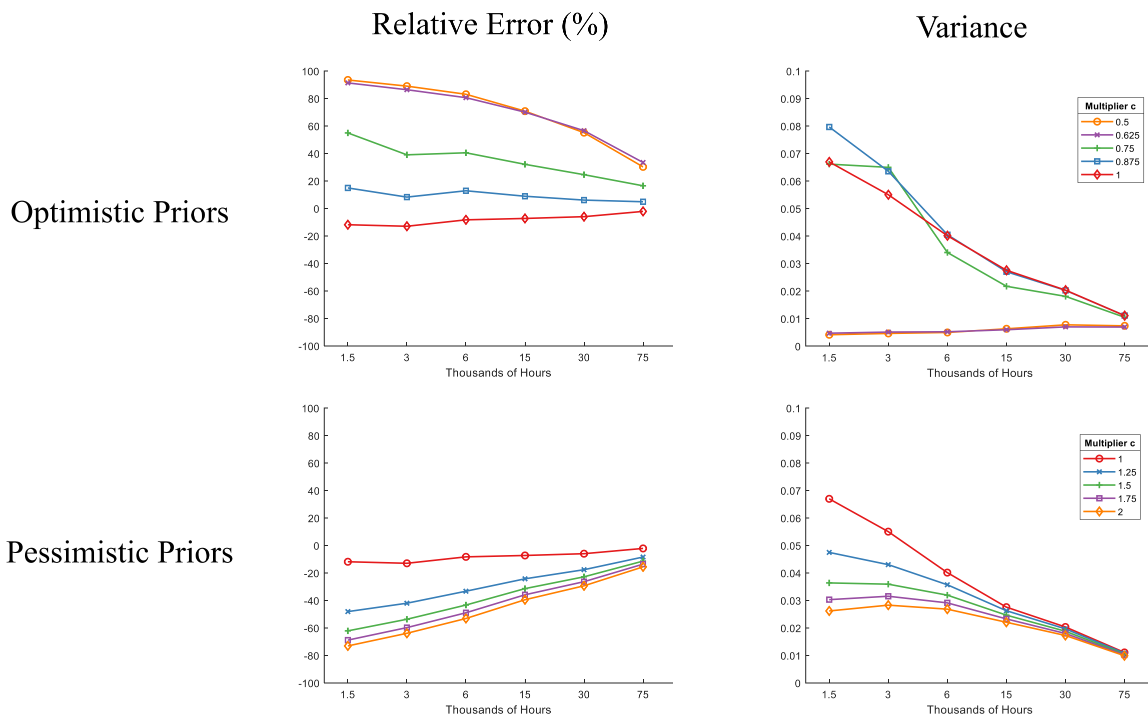

Figure 2.4: Relative error and variance of the estimate of the reliability for component A with all parameters unknown as the total testing time increases.

2.4.3 Results at System Level

Equations (2.4) and (2.5) are used to calculate the expected value and variance of each realization of system reliability, and the following equation is used to calculate the kth moment of the reliability

of each component:

$$\hat{R}_{im}^{k} = \frac{\sum_{s=1}^{N} R(\Theta_{ims})^{k}}{N} \tag{2.12}$$

Furthermore, the expected relative error and variance of the system reliability estimate are calculated in the same way as for the component.

Figure 2.5 shows the relative error and variance for the general case. The most optimistic priors are harder to correct in terms of reducing the relative error with more testing time. In contrast, the cases with pessimistic priors start with a large relative error that is significantly reduced with more testing time, however, they still present larger errors than their optimistic counterparts after testing for 75 thousand hours. This is due to the requirement that b is greater than one, which bounds the prior assessment in terms of the shape parameter requiring no reduction in the hazard rate. The variance also presents a similar behavior as in the component case. It shows reduction for all but the two most optimistic priors after 6 thousand testing hours, while the three most pessimistic cases present an increase in variance of the estimate when the testing time is less than 6 thousand hours.

Figure 2.6 shows the same results under testing environments with acceleration factors that are five times higher than the ones used in the previous example. The results show a significant reduction in the relative error for all cases with pessimistic priors as compared with their equivalents in the previous experiments. However, the cases with unbiased and optimistic priors present higher errors when the testing time is less than 15 thousand hours. In addition, the variance of the estimate increases significantly for all but the two cases with the most optimistic priors.

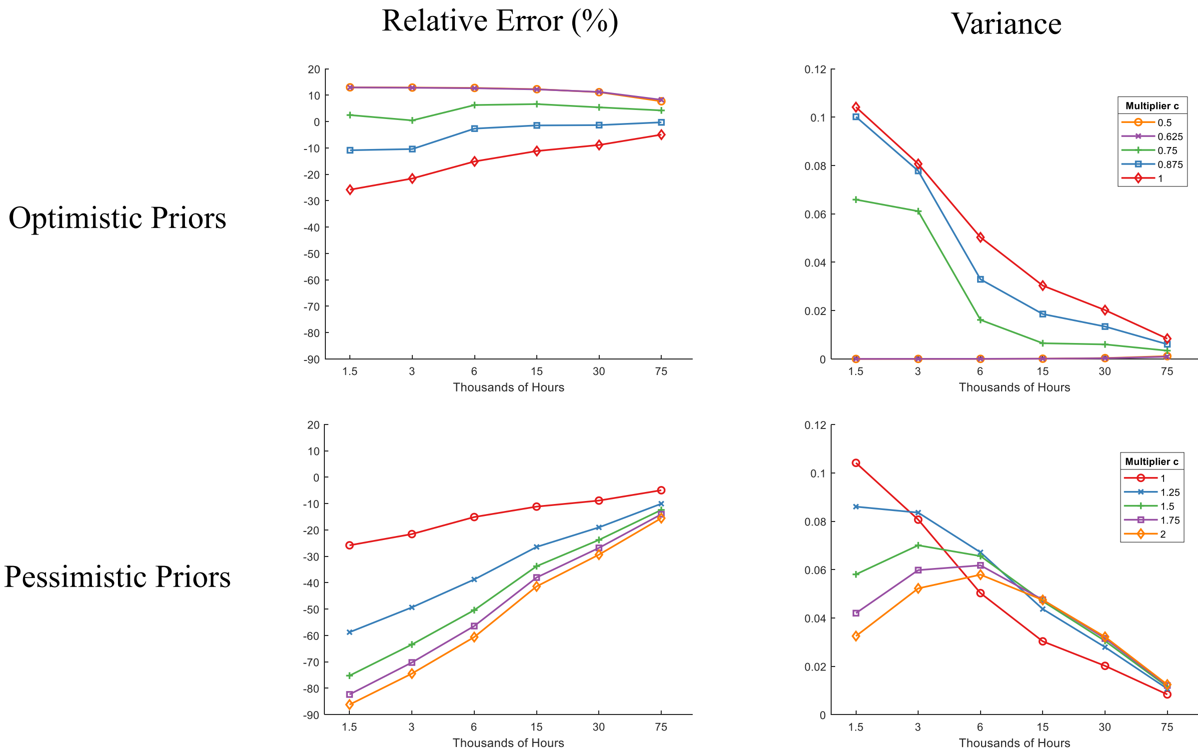

Figure 2.5: Relative error and variance of the estimate of the reliability for the system with all parameters unknown as the total testing time increases.

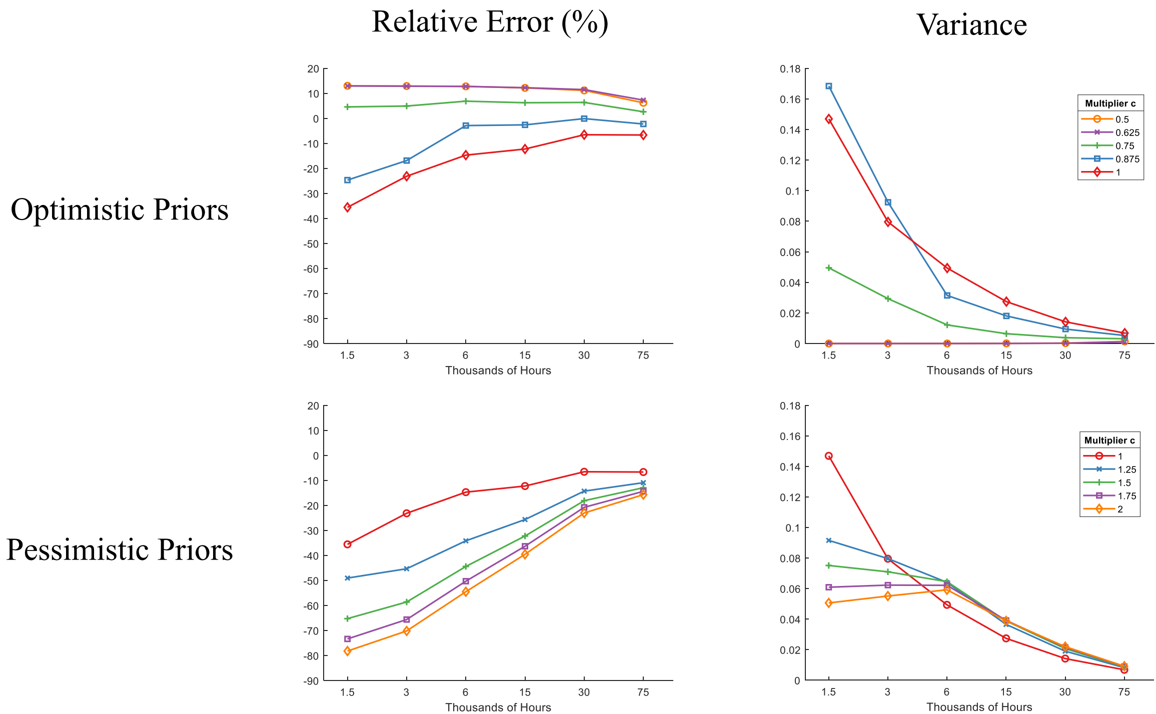

Figure 2.6: Relative error and variance of the estimate of the reliability for the system with all parameters unknown as the total testing time increases with greater acceleration factor.

In the next subsections, we present two special cases of the GBARG model when b_j is known and when both b_j and a_{jk} are known (e.g., from a physical model)

2.4.4 Case with Known Shape Parameters

This case is a straightforward application of the model presented in Section 2.3 by using Algorithm 1 while ignoring sampling from b and calculating $E[\lambda_j]$ as:

$$\begin{aligned} E[\lambda_j] &= \int_0^\infty \ln(2)\tau^{-b_j} \frac{\beta_{jt}^{\alpha_{jt}}}{\Gamma(\alpha_{jt})} \tau^{-\alpha_{jt}-1} \exp\bigg(- \frac{\beta_{jt}}{\tau}\bigg) d\tau \\ &= \ln(2) \frac{\Gamma(\alpha_{jt} + b_i)}{\Gamma(\alpha_{jt})\beta_{jt}^{b_j}} \end{aligned} \tag{2.13}$$

Figure 2.7 shows the final reliability estimate of component A as in Section 2.4.2. Unlike Figure 2.4, Figure 2.7 shows a reduction in relative error and variance for all cases compared to the case with unknown b. In addition, the variance of the estimate is reduced with more testing time for all priors. However, all cases show a convex section in the reliability estimate up to around 30 thousand testing hours. Moreover, the cases with optimistic priors show a reduction, the cases with unbiased prior stays the same, and the cases with pessimistic priors show an increase after around 75 thousand hours. Figure 2.8 presents a similar behavior for the system level results as their component level counterparts with lower initial relative errors and faster error reduction than the general model when the testing time is longer than 6 thousand hours. However, all the cases underestimate the reliability of the system due to underestimated acceleration factors that introduce a bias to overestimate the failure rates.

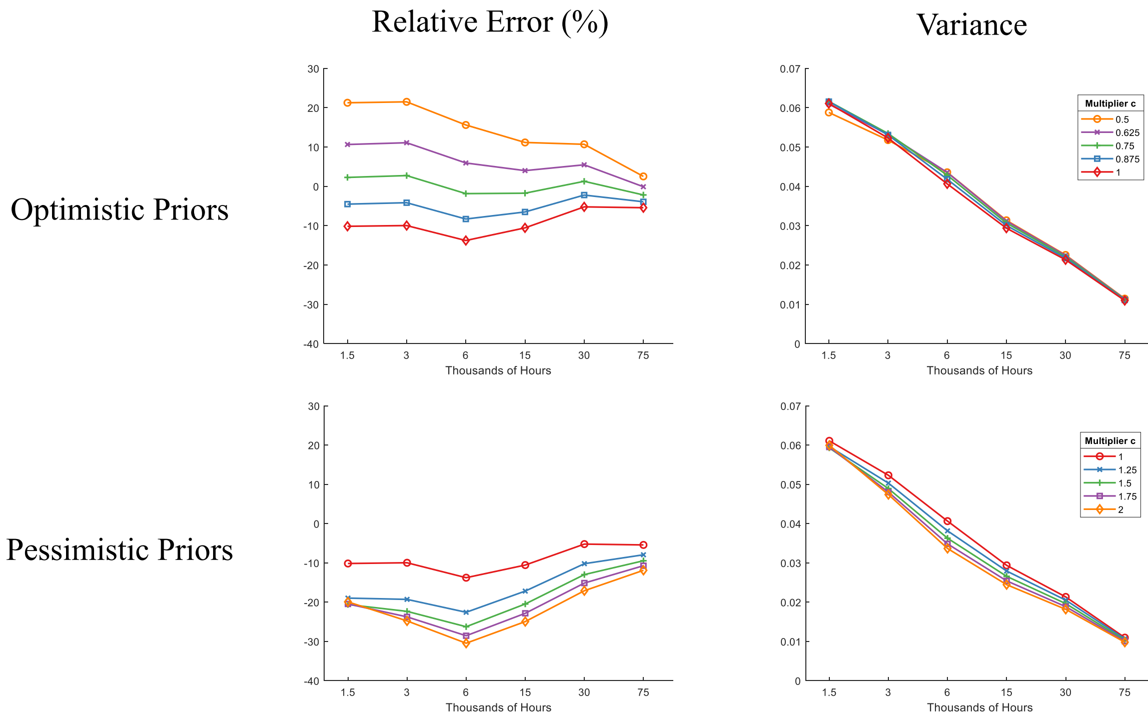

Figure 2.7: Relative error and variance of the estimate of the reliability for component A with known shape parameter (b) as the total testing time increases.

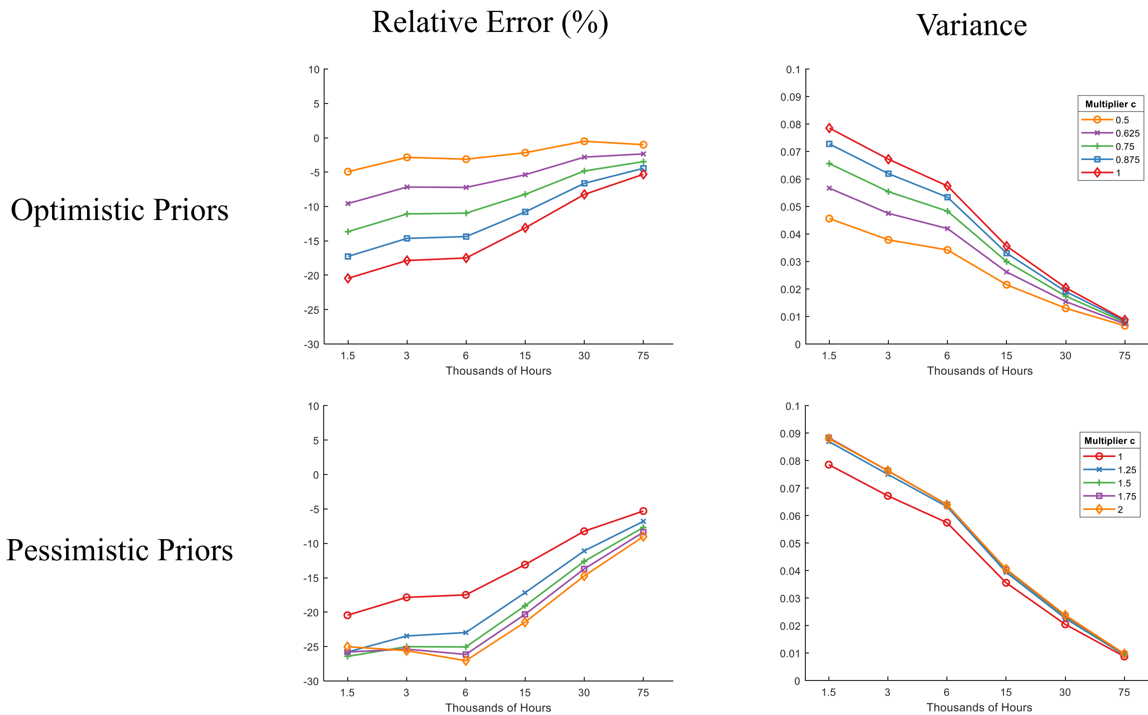

Figure 2.8: Relative error and variance of the estimate of the reliability for the system with known shape parameter (b) as the total testing time increases.

Lastly, once we know b it is easier to assess λ directly and assign a natural Gamma prior distribution to it. As a result, the sampling procedure can be simplified to a Gibbs sampler (i.e., an MH sampler with all conditional posterior distributions having closed-form expressions). However, λ still lacks a clear physical meaning which can introduce a significant bias to the elicitation process.

2.4.5 Case with Known Acceleration Factors and Shape Parameters

This case is a straightforward application of Algorithm 1 where we do not need to sample b and a. Compared to Figure 2.7, Figure 2.9 shows further improvement in the reliability estimate at the component level in terms of reduced error and variance when the acceleration factor is known. It also suggests that less testing time is required to converge to the true reliability at the system level compared to the previous models. After 15 thousand hours of testing, the difference in the point estimate of the reliability is the same for all pessimistic priors such that only the new data seems to matter, and the variance of the reliability estimate is similar across all cases. After seventy five thousand hours, the reliability estimate generated for each prior is withing 5% relative error from the true reliability.

Figure 2.10 shows results for the system level reliability estimate. The general behavior is similar to the one at the component level with a lower relative error and variance as compared to Figures 2.5 and 2.8. In addition, the relative errors of the final estimates are less than 5% for all testing times. Finally, the reliability estimate tends to improve faster for the cases with optimistic priors while it starts with a low error for the cases unbiased and pessimistic priors.

2.5 Alternative Approaches

In this section, we present an alternative approach to incorporate prior information on the parameters of the life-time distribution, and alternative models for estimating each a_{jk}. We assume that the models treat only components and omit the i index in our notation.

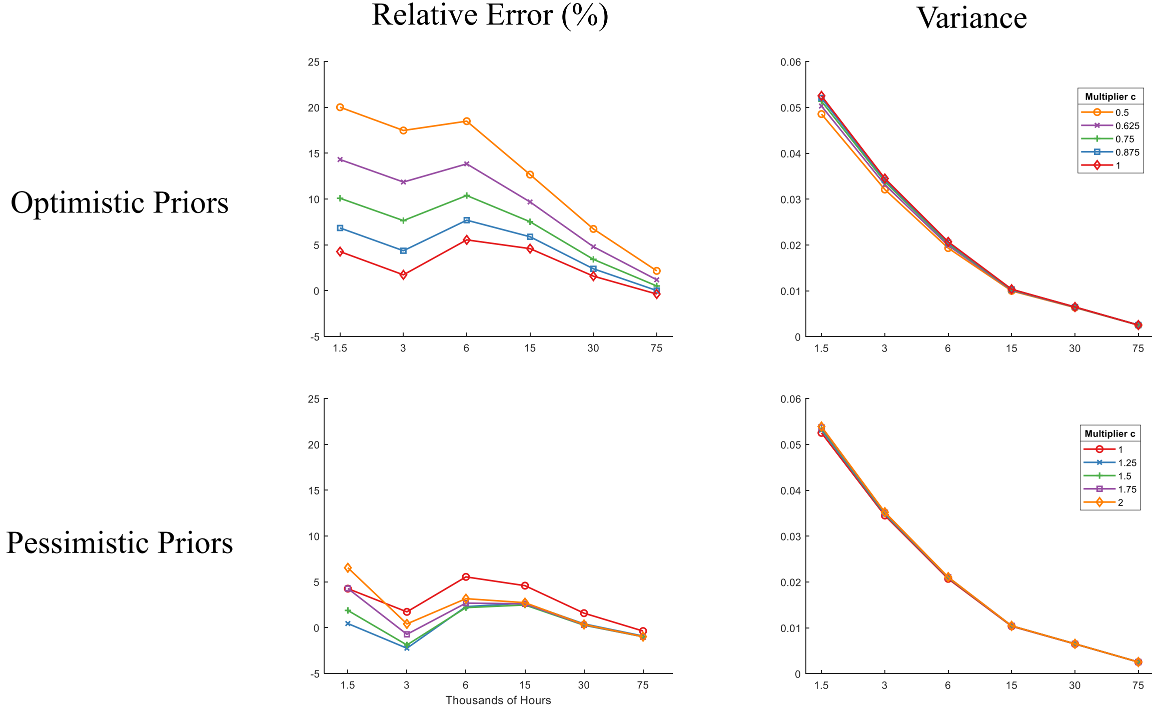

Figure 2.9: Relative error and variance of the estimate of the reliability for component A with known shape parameter and acceleration factors as the total testing time increases.

2.5.1 Alternative Approach for Prior Information on the Lifetime Distribution

Soland (1969) developed a conjugate prior distribution when both of the Weibull parameters are unknown by restricting b_j to take fixed values b_{jv}, for $v = 1, \cdots, V_j$, and assigning a prior probability mass function (pmf) for each b_{jv}. In other words, the range of b_j is reduced to a finite number of fixed points and a probability is assigned to each point. The prior distribution is of the form:

$$\pi(\lambda_j, b_j) = \pi(\lambda_j | b_j)\pi(b_j), \tag{2.14}$$

where $\pi(b_j) = P\{b_j = b_{iv}\}$ and $\pi(\lambda_j|b_j)$ follows a Gamma distribution. We use p_{jvs} as shorthand notation for $P\{b_j = b_{iv}\}$ after s stages.

This prior distribution implies that for each failure mode j we need to calculate V_j posterior distributions for $(\lambda_j|b_j)$ using the results from Section 2.2 with $b_j = b_{jv}$. The posterior pmf is

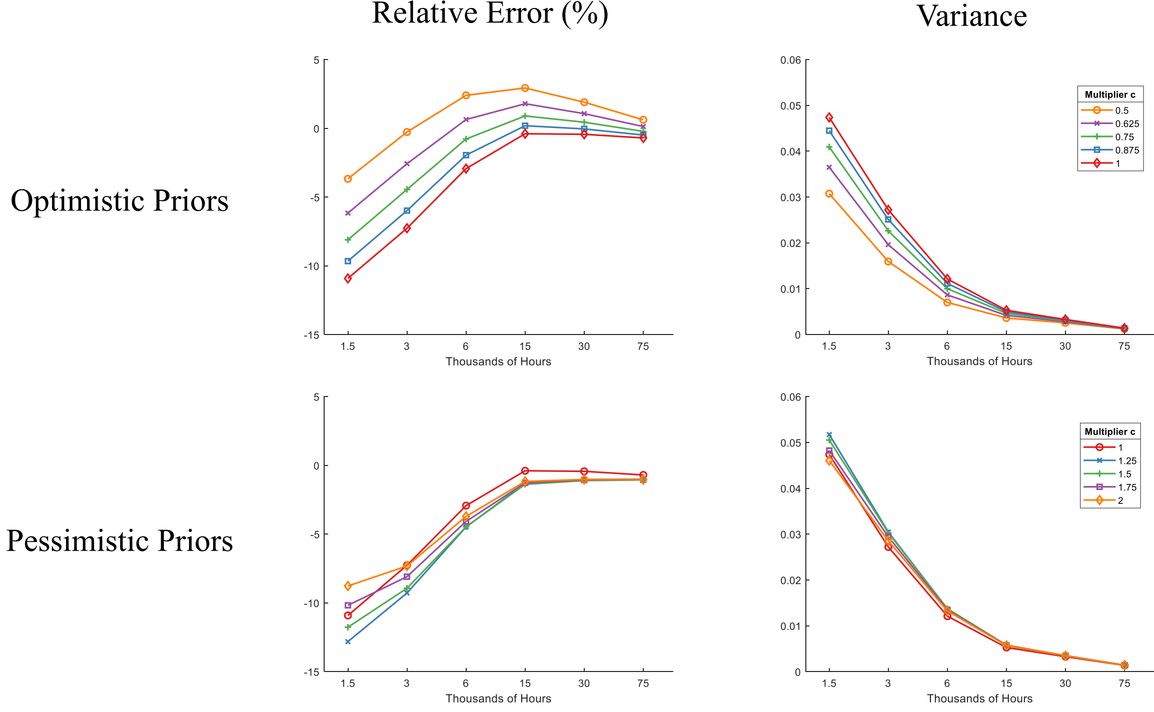

Figure 2.10: Relative error and variance of the estimate of the reliability for the system with known shape parameter and acceleration factors as the total testing time increases.

calculated as:

$$p_{jvs} = \frac{p_{jvs-1}(a_j b_{jv})^{\sum_w \delta_{jws}} \beta_{jvs-1}^{\alpha_{jvs-1}} \left(\prod_w t_w^{\delta_{jws} b_{jv}}\right) \Gamma(\alpha_{jvs}) / \beta_{ivs}^{\alpha_{jvs}} \Gamma(\alpha_{jvs-1})}{\sum_v p_{jvs-1}(a_j b_{jv})^{\sum_w \delta_{jws}} \beta_{jvs-1}^{\alpha_{jvs-1}} \left(\prod_w t_w^{\delta_{jws}}\right)^{b_{jvs-1}} \Gamma(\alpha_{jvs}) / \beta_{jvs}^{\alpha_{jvs}} \Gamma(\alpha_{jvs-1})}. \tag{2.15}$$

Lastly, the moments of the reliability of a component for a target life T can be calculated by:

$$E[R^m] = \prod_{j=1}^{n_i} E\left[r_j^m\right] = \prod_{j=1}^{n_i} \left[\sum_{v=1}^{V_j} E\left[r_j^m | b_j\right] p_{jvs}\right] = \prod_{j=1}^{n_i} \left[\sum_{v=1}^{V_j} \left(\frac{\beta_{jvs}}{\beta_{jvs} + mT^{b_{jv}}}\right)^{\alpha_{jvs}} p_{jvs}\right]. \tag{2.16}$$

We simulated 1000 replications of a reliability growth program for component A as in Section 2.4 with known a and d, and $\lambda_{jv}|b_{jv}$ having a Gamma(α_{jv}, β_{jv}) prior distribution where $\alpha_{jv} = 2$ for all failure modes and $\beta_{jv} = \sqrt{r_j} T^{b_{jv}}/(1 - \sqrt{r_j})$. We consider 10 equally spaced values between 1.20 and 1.60 for b_{jv} on both failure modes with equal initial probability of 0.10. Table 2.4 shows the probabilities associated with each b_{jv} which tend to converge around the true b_i (i.e., 1.52 and

1.23, respectively), as the testing time increases. Moreover, Figure 2.11 presents a box plot with the expected value of the final reliability as the testing time increases. The results show that the relative error and variance of the final estimate decrease as the testing time increases. However, this is not the case for 75 thousand hours due to observing numerical errors in calculating the pmf for b_1 on 951 out of 1000 replications with this testing time. Such numerical errors are produced by the overflow of our computer when β and α are too large. Noting the computational difficulty in applying this method for only uncertainty on the life-time parameters, we anticipate that there would be significant challenges in incorporating additional uncertainty in other parameter into this approach.

Table 2.4: Pmf for the shape parameter b_j.

Failure	Shape	Testing Time (Thousands of hours)					
Mode j	Parameter (b)	1.5	3	6	15	30	75
1	1.22	0.053	0.027	0.012	0.004	0.001	0.000
	1.26	0.064	0.042	0.025	0.012	0.005	0.000
	1.30	0.077	0.062	0.046	0.030	0.017	0.003
	1.34	0.091	0.084	0.075	0.060	0.043	0.015
	1.38	0.104	0.108	0.107	0.099	0.083	0.047
	1.42	0.116	0.127	0.135	0.137	0.130	0.107
	1.46	0.124	0.140	0.154	0.165	0.169	0.177
	1.50	0.127	0.144	0.159	0.175	0.191	0.224
	1.54	0.125	0.139	0.152	0.169	0.190	0.229
	1.58	0.118	0.127	0.136	0.150	0.171	0.198
2	1.22	0.156	0.176	0.193	0.212	0.232	0.270
	1.26	0.147	0.163	0.178	0.193	0.207	0.230
	1.30	0.135	0.147	0.156	0.165	0.170	0.177
	1.34	0.123	0.128	0.131	0.132	0.131	0.125
	1.38	0.109	0.108	0.105	0.101	0.095	0.083
	1.42	0.094	0.088	0.081	0.073	0.065	0.051
	1.46	0.079	0.069	0.060	0.051	0.044	0.031
	1.50	0.065	0.053	0.043	0.035	0.028	0.017
	1.54	0.052	0.039	0.030	0.023	0.018	0.010
	1.58	0.041	0.028	0.021	0.015	0.011	0.005

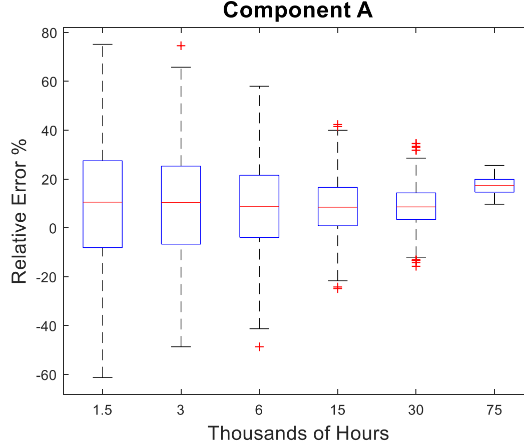

Figure 2.11: Relative error of the reliability estimate for component A under discretized shape parameter as the total testing time increases.

2.5.2 Estimation of Acceleration Factors

For a fixed b_j, the transformation $\tau = t^{b_j}$ follows an exponential distribution. If we assume the acceleration factor $a_j(z)$ depends on covariates z of a testing environment and the specific failure mode, it can be shown that a time contraction ${}^{\tau_j}/_{a_j}$ is equivalent to an increased rate parameter $\gamma_j = a_j\lambda_j$. Under this condition, by assuming that a_j is a fixed value given z, it can be estimated by deriving the distribution of ${}^{\gamma_j}/\lambda_j$. Thus, using the posterior distribution of λ_j and γ_j, a_j follows a Beta Prime distribution with pdf:

$$f(a_j) = \frac{1}{B(\alpha_{\gamma_j}, \alpha_{\lambda_j})} \frac{\beta_{\gamma_j}}{\beta_{\lambda_j}} \left(1 + \frac{\beta_{\gamma_j} a_j}{\beta_{\lambda_j}}\right)^{-(\alpha_{\gamma_j} + \alpha_{\lambda_j})} \left(\frac{\beta_{\gamma_j} a_j}{\beta_{\lambda_j}}\right)^{\alpha_{\gamma_j} - 1}.$$

Furthermore, the expected value and variance of a_j are:

$$E\left[a_j\right] = \frac{\beta_{\lambda_j}}{\beta_{\gamma_j}} \frac{\alpha_{\gamma_j}}{\alpha_{\lambda_j} - 1}, \tag{2.17}$$

$$\text{Var}(a_j) = \frac{\beta^2_{\lambda_j}}{\beta^2_{\gamma_j}} \frac{\alpha_{\gamma_j}(\alpha_{\gamma_j} + \alpha_{\lambda_j} - 1)}{(\alpha_{\lambda_j} - 2)(\alpha_{\lambda_j} - 1)^2}. \tag{2.18}$$

This shows that $\alpha_{\lambda_j} > 2$ and $\alpha_{\gamma_j} > 0$ in order to guarantee meaningful posterior point estimates when no failures are observed in any or both testing conditions. Moreover, this method can be

easily modified to handle a joint prior distribution for (λ, b) using the ideas in Section 2.5.1.

2.6 Conclusions

A new Bayesian framework for analyzing the results from accelerated reliability growth tests with multiple uncertainties is developed in this paper. A general MH procedure is developed to analyze the test results under a constant-stress ALT model, in which no explicit life-stress relationship is assumed. Moreover, a block-decomposition approach is utilized to aggregate the component-level reliability estimates for obtaining the point estimate of the reliability of the system when no new failure modes arise from interactions between components. Numerical studies illustrate the effectiveness of the Bayesian framework in the estimation of the system reliability with multiple test-correction stages as the testing time increases. In particular, the impact of various bias levels of informative prior distributions of the model parameters is investigated. As expected, the framework requires more testing data to correct the bias of overly optimistic prior information. Furthermore, use of testing environments with higher acceleration factors does not guarantee significant improvements on the reliability estimates when a short amount of testing time is applied, specially if the prior assessments of the reliability are too cautious.

In addition, special cases are considered when the shape parameter of the lifetime distribution and/or acceleration factors are known. In practice, these parameters can be obtained from physical models. Numerical experiments illustrate significant reductions in both bias and variance of reliability estimates, and faster convergence to the true reliability with more testing time when such parameters are known, especially the shape parameter. Moreover, the posterior sample of the model parameters can be used to evaluate the effectiveness of using a predetermined stress environment for ALT and corrections in reducing the rate parameter.

In practice, the proposed framework can be extended to incorporate failure modes presented only at the system level by using pseudo components that represent interactions among the components. Moreover, it can be used to perform resource allocation and develop decision rules for determining when to stop testing for applying corrections or declaring the reliability objective as

achieved. Such rules can be used to test if the prior information is overly optimistic or pessimistic by noting that little or no testing may be required to make a decision. Another interesting line of research is the development of an MH algorithm that incorporates an explicit life-stress relationship, such as a power rule, and study the impact of such a change in the performance of different frameworks when multiple stresses are used.

References

Acevedo, P. E., Jackson, D. S., & Kotlowitz, R. W. (2006). Reliability growth and forecasting for critical hardware through accelerated life testing. *Bell Labs Technical Journal*, *11*(3), 121–135.

Crow, L. H. (2004a). An extended reliability growth model for managing and assessing corrective actions. In *2004 Proceedings Annual Reliability and Maintainability Symposium - RAMS*, (pp. 73–80).

Crow, L. H. (2004b). An extended reliability growth model for managing and assessing corrective actions. In *2004 Proceedings Annual Reliability and Maintainability Symposium - RAMS*, (pp. 73–80).

Elsayed, E. (2012). Overview of reliability testing. *IEEE Transactions on Reliability*, *61*(2), 282–291.

Feinberg, A. (1994). Accelerated reliability growth models. *Journal of the IES*, *37*(1), 17–23.

Freels, J. K., Pignatiello, J. J., Warr, R. L., & Hill, R. R. (2015). Bridging the gap between quantitative and qualitative accelerated life tests. *Quality and Reliability Engineering International*, *31*(5), 789–800. QRE-13-0158.R1.

Hamada, M. S., Wilson, A. G., Reese, C. S., & Martz, H. F. (2008). *Bayesian reliability* (1 ed.). Springer New York.

Jiang, P., Lim, J.-H., Zuo, M. J., & Guo, B. (2010). Reliability estimation in a Weibull lifetime distribution with zero-failure field data. *Quality and Reliability Engineering International*, *26*(7), 691–701.

Jin, T. & Coit, D. W. (2008). Unbiased variance estimates for system reliability estimate using block decompositions. *IEEE Transactions on Reliability*, *57*(3), 458–464.

Martz, H. & Waller, R. (1991). *Bayesian reliability analysis* (1 ed.). Krieger Publishing Company.

Martz, H. F. & Waller, R. A. (1990). Bayesian reliability analysis of complex series/parallel systems of binomial subsystems and components. *Technometrics*, *32*(4), 407–416.

Meeker, W. & Escobar, L. (1998). *Statistical methods for reliability data*. John Wiley & Sons, New York, New York.

Nelson, W. (1990). *Accelerated testing - statistical models, test plans, and data analysis*. John Wiley & Sons, Hoboken, New Jersey.

Pollock, S. M. (1968). A Bayesian reliability growth model. *IEEE Transactions on Reliability*, *R-17*(4), 187–198.

Ruiz, C., Liao, H., Pohl, E., & Sullivan, K. (2018). Bayesian accelerated reliability growth of complex systems. In *2018 Proceedings Annual Reliability and Maintainability Symposium - RAMS*.

Singpurwalla, N. D. (2011). *Reliability and Risk: A Bayesian Perspective* (1 ed.). John Wiley & Sons, Inc.

Soland, R. M. (1969). Bayesian analysis of the Weibull process with unknown scale and shape parameters. *IEEE Transactions on Reliability*, *18*(4), 181–184.

Somerville, I. F., Dietrich, D. L., & Mazzuchi, T. A. (1997). Bayesian reliability analysis using the Dirichlet prior distribution with emphasis on accelerated life testing run in random order. *Nonlinear Analysis: Theory, Methods & Applications*, *30*(7), 4415–4423.

Strunz, R. & Herrmann, J. W. (2012). Planning, tracking, and projecting reliability growth a Bayesian approach. In *2012 Proceedings Annual Reliability and Maintainability Symposium - RAMS*, (pp. 1–6).

Thompson, W. E. & Haynes, R. D. (1980). On the reliability, availability and Bayes confidence intervals for multicomponent systems. *Naval Research Logistics Quarterly*, *27*(3), 345–358.

Van-Dorp, J. R. & Mazzuchi, T. A. (2004). A general Bayes exponential inference model for accelerated life testing. *Journal of Statistical Planning and Inference*, *119*(1), 55 – 74.

Wayne, M. & Ellner, P. (2010). A comparison of the robustness of reliability growth assessment techniques. In *2010 Proceedings Annual Reliability and Maintainability Symposium - RAMS*, (pp. 1–6).

Wayne, M. & Modarres, M. (2015). A Bayesian model for complex system reliability growth under arbitrary corrective actions. *IEEE Transactions on Reliability*, *64*(1), 206–220.

Yuan, T., Liu, X., Ramadan, S. Z., & Kuo, Y. (2014). Bayesian analysis for accelerated life tests using a Dirichlet process weibull mixture model. *IEEE Transactions on Reliability*, *63*(1), 58–67.

3 A Non-parametric Degradation-based Method for Modeling Reliability Growth

The competitiveness of the modern business environment creates a need for shortening the development time while assuring high product reliability. In addition, recent technological advancements in sensor technology and data acquisition have made it possible to continuously monitor the health status or performance of a product during testing. Using such condition monitoring data, the designer can model the degradation process of this product and provides an informative and accurate tool for failure analysis and reliability estimation. Recently, much attention has been focused on developing new reliability growth methods in hopes of speeding up product development in a cost-effective way. To this end, accelerated testing can be conducted in a reliability growth program. One way to take advantage of both accelerated testing and degradation analysis for reliability growth is to conduct accelerated degradation testing (ADT).

3.1 Introduction

Today's highly competitive business environment, driven by continuous technological advancements and consumers' increasing expectations on product reliability, creates a need for shortening the development time while continuing to assure high product reliability. To meet the requirements, a variety of techniques and data analysis methods have been developed. In particular, recent technological advancements in sensor technology and data acquisition have made it possible to continuously monitor the health status or performance of a product during testing and operation. Using such condition monitoring techniques, the product developer can create a degradation index to model the degradation of the product over time. As an important alternative to failure time data analysis, failure analysis and reliability estimation based on degradation data would be more informative and accurate (Hamada, 2005).

Recently, special interests have been focused on the development of new reliability growth methods in hopes of speeding up product development in a cost-effective way. A reliability growth program consists of multiple stages of testing a product and incorporating corrective actions to re-

duce the frequency of failures (Crow, 2004), and accelerated testing can be conducted to reduce the testing time required for a reliability growth program by using statistical or physics based methods to analyze the test results (Krasich, 2014). One way to take advantage of both accelerated testing and degradation analysis for quick reliability growth is to conduct accelerated degradation testing (ADT). ADT data analysis has been extensively studied using parametric and nonparametric models since the 1960's (Nelson, 1990). However, to the best of our knowledge, no research has been conducted on reliability growth via ADT. It would be invaluable for practitioners to use a new method that efficiently incorporates ADT and data analysis into a reliability growth program. Among various possible approaches, to assist practitioners in modeling complex degradation processes, an attractive feature of such a method would be to use a non-parametric degradation model that can avoid model misspecification in the reliability growth program.

This paper proposes a non-parametric degradation-based method for modeling reliability growth. To the best of our knowledge, this is the first attempt in modeling reliability growth via degradation analysis in a non-parametric way. The new method avoids possible misspecifications of underlying failure time distribution and parametric degradation model. We show how to utilize degradation data with functional data analysis and Gaussian processes to predict the MTTF and reliability of a product given a degradation level. The model can incorporate all types of stress profiles, such as ramp stress and step stress.

The remainder of this paper is organized as follows. In Section 3.2, we describe a multi-stage reliability growth program and the degradation data that we expect to observe. In Section 3.3 we present a degradation-based method to model reliability growth. In Section 3.4, we assess the efficacy of the proposed method to estimate reliability of a product after corrective actions have been applied under monotone and non-monotone degradation process assumptions. We summarize our results and present conclusions in Section 3.5.

3.2 Degradation-based Reliability Growth

Assume a product's performance can be tracked through a signal Y and that it is considered failed if its performance surpasses a known threshold y^f, for this paper we assume that y is positive and that y^f is equal to 100. We consider a reliability growth program consisting of S stages of testing of identical copies of a product with corrective actions at the end of each stage such that the degradation of the product slows down after corrections if they are effective. Moreover, ADT speeds up the degradation of a part and multiple testing environments can be used during each testing stage. As an example, Figure 3.1 shows the degradation paths of units during the first two stages of testing. Starting from the left, we observe 5 units under ADT which shows a faster degradation rate than the next 5 units tested under use condition; the last 5 units are tested under use condition after corrections have been applied and show a slower rate of degradation.

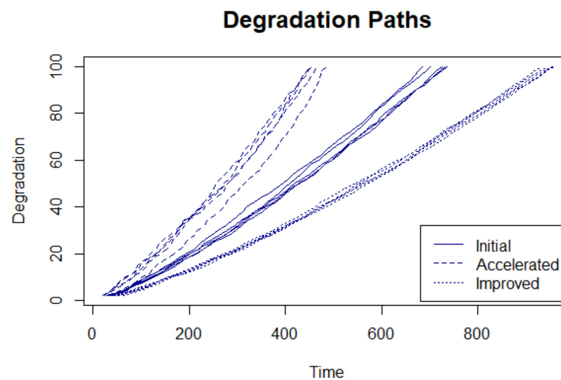

Figure 3.1: Observed degradation for units tested during a reliability growth program.

However, such data introduces complications for constructing a non-parametric degradation model in the form of truncated observations due to reduction in the number of units tested at higher test times. In order to construct a good non-parametric model, we need to divide the time scale in intervals to model the degradation changes and this creates an imbalanced estimate since each unit has its own failure time which means that as the time increases we less signals to work with and it becomes difficult for the model to predict the life-time of units that last more than the observed failure times. One alternative to tackle this problem is to scale the observations such that each

signal goes through a common time frame, but such procedure fundamentally changes the data and may introduce some biases. Alternatively, another approach, suggested in (Zhou et al., 2012), is to shift the signal axis such that time is predicted based on degradation signal. Figure 3.2 presents the same data as in Figure 3.1 with the axis changed such that now the data is not censored and the non-parametric model can be estimated for any life-time results as long as all units are tested to failure or to some upper degradation level. Thus, the second approach eliminates the need to transform the data and it can be used to predict the time-to-signal of any unit and for a defined degradation threshold it can predict the mean time to failure (MTTF) of the part.

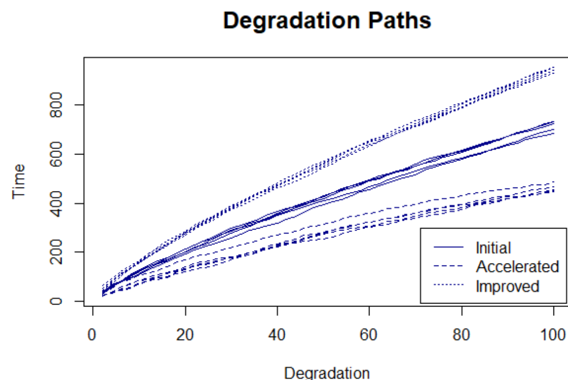

Figure 3.2: Time to observe a degradation level.

3.3 Non-parametric Degradation Modeling

In this section, we present the non-parametric statistical model to estimate the reliability of a component after multiple testing stages based on degradation measurements. We assume a component has a known degradation process with signal Y such that it fails if the degradation signal surpasses a known threshold y^f. We treat the degradation path of each tested unit as a realization of a stochastic process and estimate the mean function for the time-to-signal using functional data analysis (FDA). Moreover, the variation between the signal of each individual unit and the mean function is captured by a Gaussian process (GP). This joint framework is known as Gaussian process functional regression (GPFR) [4]. The general model describing the behavior of the time z_i to achieve

a degradation level y_j for unit i is:

$$z_i(y_j) = \mu_i(y_j, u_i) + \tau_i(x_i) + \epsilon_i(y_j) \tag{3.1}$$

where y_j is the jth element of a $p-$demensional vector y of degradation levels chosen to characterize the process, μ_i is the mean function that depends on the degradation level and n scalar covariates u_i (under constant-stress levels and corrective actions done before testing), x_i is a functional regressor that includes the degradation points y_j and the level of time-varying stressors applied during testing at the time of each measurement, $\tau_i(x_i)$ defines the covariance structure of $z_i(y_j)$ and is modeled by a Gaussian Process (GP) with mean 0 and covariance defined by a kernel $k_i(\cdot)|x_i$ with parameter θ_i, and ϵ_i is the measurement error that is assumed to follow a normal distribution with mean 0 and variance σ_ϵ^2. Following the results on (Shi & Choi, 2011), the model parameters are computed using a two-stage process. First, a linear functional model is used to estimate the mean function with:

$$z_i(y_j) \approx \tilde{z}_i(y_j) = A_i^T \Omega_j \tag{3.2}$$

$$\mu_i(y_j, u_i) = u_i^T B^T \Omega_j \tag{3.3}$$

where Ω_j is a vector of h basis functions evaluated at y_j, A_i is an $h-$dimensional vector of coefficients, and B^T is an $h \times n$ matrix of basis coefficients.

For the second stage, let $\tau_i(x_i)$ be approximated by $\tau_i(x_i) = z_i(y_j) - u_i^T B^T \Phi(y_j)$ such that if we have p observations for unit m, then

$$\tilde{\tau}_i(x_i) = (\tilde{\tau}_{i1}, \ldots, \tilde{\tau}_{ip}) \sim N(0, \Psi_i) \tag{3.4}$$

where $\Psi_{ijl} = k_i(x_{ij}, x_{il}; \theta_i) + \sigma_\epsilon^2$.

The estimation process requires an initial estimate of θ_i in order to compute $\hat{\Psi}_i$. Then, the mean

parameters can be estimated as:

$$\hat{A}_i = \left(\Omega_j^T \hat{\Psi}_i \Omega_j + \lambda_i R\right)^{-1} \Omega_j^T \hat{\Psi}_i z_i \tag{3.5}$$

$$v(\hat{B}_i^T) = \left(J \otimes U^T U + \lambda_2 R \otimes I\right)^{-1} v\left(U^T A J\right) \tag{3.6}$$

where z_i is the vector of observed times for unit i, λ is a regularization parameter chosen by cross-validation, $v(\cdot)$ denotes the vector of length $p \times h$ formed by stacking the columns of a matrix, $\otimes$ is the Kronecker product of two matrices, $J = \int \Phi(y)\Phi(y)^T dy$, and U is the matrix of observed scalar covariates for the M units tested. Then, we can estimate θ_i given the current $\tau_i(x_i)$ and repeat the estimation process until a convergence criteria is satisfied.

The population reliability after observing M units for a target time z^f, covariates under use condition u_0 and x_0 can be estimated by first computing the unit mean and variance functions as

$$z_i^* = \mu_0^T \hat{B}^T \Upsilon(y^f) + H^T \left(y_i - \mu_i^T \hat{B}^T \Upsilon(y^f)\right) \tag{3.7}$$

$$\hat{\sigma}_i^{*2} = \hat{\sigma}_{GP}^{*2} \left(1 + u_0^T (U^T U)^{-1} u_0\right) \tag{3.8}$$

where $\hat{\sigma}_{GP}^{*2}$ is computed as $\Psi_i(x^f, x^f) - H^T \Psi_i(x_0, x_0) H$, H is the matrix resulting from $\Psi_i(x^f, x_m)\Psi_i(x^f, x^f)^{-1}$, and x^f is the vector of variable covariates at use condition. Thus, we can calculate the reliability of a population as:

$$P\{z(y^f) < z^f\} = \Phi\left(\frac{z^f - \hat{z}^*}{\hat{\sigma}^*}\right) \tag{3.9}$$

where $\hat{z}^* = \sum_{i=1}^M z_i^*/M$, $\hat{\sigma}^{*2} = \sum_{i=1}^M \hat{\sigma}_i^{*2}/M + (\sum_{i=1}^M \hat{z}_i^{*2}/M - \hat{z}^{*2})$, $\Phi(\cdot)$ is the cumulative distribution function (cdf) of the standard normal distribution. Note that $\hat{\sigma}^{*2}$ depends on an empirical estimate of the variance structure which is captured in $\hat{\sigma}_{GP}^{*2}$ based on the parameters fitted for each unit tested and the expected conditions for the unit populations. In addition, those estimates can be used to predict the RUL of a unit by including the already observed covariates and degradation measurements in the prediction.

3.4 Numerical Example

In this section, we conduct a simulation study to assess the performance of the proposed methodology to estimate the reliability of a population after corrections. We simulate two types of degradation paths; monotone increments generated from an Inverse Gaussian process (IGP) (Ye & Chen, 2014) with parametrization as in Equation 3.10, and, non-monotone increments generated from a Wiener process (WP) (Wang, 2010) with parametrization as in Equation 3.11.

$$f(\Delta y_{ij}) = \sqrt{\frac{\lambda \Delta h_{ij}^2}{2\pi \Delta y_{ij}^3}} \exp\left(\frac{-\lambda}{2\Delta y_{ij} - \mu^2} \left(\Delta y_{ij} - \mu \Delta h_{ij}\right)^2\right) \tag{3.10}$$

$$f(\Delta y_{ij}) = \phi\left(\frac{\Delta y_{ij} - \mu \Delta h_{ij}}{\sigma \Delta h_{ij}}\right) \tag{3.11}$$

where $\Delta y_{ij} = y_{ij} - y_{ij-1}$, $\Delta h_{ij} = h(z_{ij}) - h(z_{ij-1})$, h is a monotone time transformation, for this example $h(z) = z^{\eta}$, and $\phi(\cdot)$ is the probability density function (pdf) of the standard normal distribution.

3.4.1 Degradation Characteristics and Data Generation Process

All simulation experiments are done using two stages of testing, i.e. $S = 2$, with one correction at the end of the first stage. During each stage, 5 units are tested under use condition and 5 under fixed stress ADT, i.e. the stressors are set at the highest stress possible for the duration of the test such that we only have scalar covariates and all units are tested until failure. Table 3.1 shows two sets of parameters used for our experiments, the first set is for presentation convenience of the confidence intervals for the mean time-to-signal function, and the second set is for estimating the reliability of a highly reliable products. The only parameter affected by ADT or corrective actions is the mean degradation μ_i^s where the subscript i equals 1 if ADT is applied, 0, otherwise, and the superscript s is the testing stage.

We simulate the results by setting the observed increments to be $\Delta y_j = {}^{y^f}\!/_{n}$ where n is the desired number of observations on each degradation path and y^f is the failure threshold. In each

Table 3.1: Parameters used on the experiments

Parameter	Plots		Reliability	
	IGP	WP	IGP	WP
μ_0^1	0.2	0.2	0.02	0.02
λ, σ	0.5	1.41	0.05	4.47
η	1.2	1.2	1.2	1.2
μ_1^1	0.37	0.37	0.037	0.037
μ_0^2	0.167	0.167	0.016	0.016
μ_1^2	0.254	0.254	0.025	0.025

testing stage, we sample the first passage time z_{ij} by first generating n replications of the time transformation increments Δh_{ij} required to observe a degradation increment of Δy_j by numerically computing the inverse cdf for the IGP given a randomly generate uniform number. Then, we compute $h_{ij} = \sum_{k=1}^{j} \Delta h_{ij}$ and $z_{ij} = \sqrt[\eta]{h_i j}$. For generating data from an WP, we sample an IGP with parameters (μ, σ^{-1}) since and IG distribution is the well-known first passage time of a Brownian motion process with drift. The generated data is then analyzed using the methodology presented in the previous section.

3.4.2 Results

In order to train the model, covariates u_i are incorporated in the form as a four dimensional vector with elements δ_{ic} for $c = 1, \ldots, 4$; and $\delta_{i1} = 1$, for all units in order to capture the baseline mean function of the time-to-signal process; $\delta_{i2} = 1$, if ADT before corrections is used for unit i, 0, otherwise; $\delta_{i3} = 1$, if corrections are applied before testing unit i, 0, otherwise; $\delta_{i4} = 1$, if ADT after corrections is used for unit i, 0, otherwise.

We begin by exploring the effects the number of measurements n on the estimation of the mean function when the degradation process is monotone. First, Figure 3.3 shows the 95% confidence interval for the mean time-to-signal using 50 measurements per unit tested, it is clear that the model estimates the mean function satisfactorily. On the other hand, Figure 3.4 presents the results of analyzing the same degradation path with only 25 measurements per unit tested, the results show an almost identical performance to training the model with 50 observations per unit. Those results

suggest that the performance of the model is not significantly affected by down sampling the original data set during the training process such that if computational time is an issue it is possible to safely reduce the size of the data set in order to reduce computations.

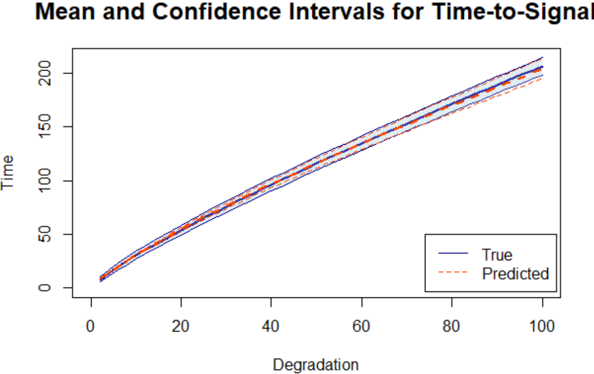

Figure 3.3: Mean time to degradation function with 50 measurements.

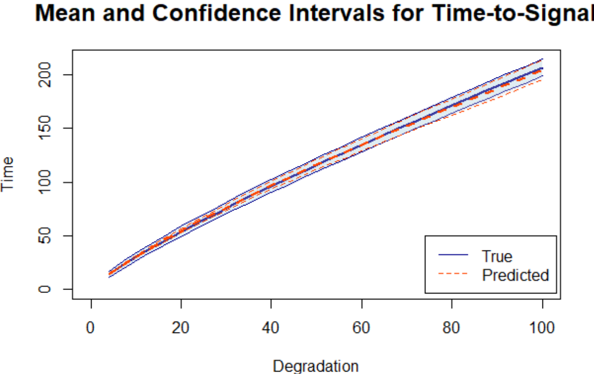

Figure 3.4: Mean time to degradation function with 25 measurements.

Second, we generate data from a WP and train the model using 50 measurements. Figure 3.5 presents the results using the same amount of units as in the IGP case, it is evident that more units are needed to get a good estimate of the mean time-to-signal function since such a process is non-monotone. In experiments not presented here, we required at least 20 units for each testing environment in each testing stage to get a satisfactory performance, which is four times the amount of data required for the monotone degradation case.

Lastly, we compare the reliability functions from the non-parametric method with that of a

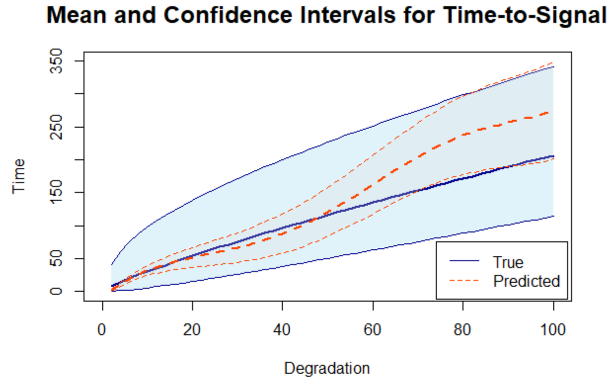

Figure 3.5: Mean time to degradation function with 50 measurements.

parametric model. As parametric model, we fit a Weibull distribution with the following pdf:

$$f(t) = \frac{\beta}{\alpha d\eta}\left(\frac{t}{\alpha d\eta}\right)^{\beta-1} \exp\left(\left[\frac{t}{\alpha d\eta}\right]^{\beta}\right) \tag{3.12}$$

where β is the shape parameter, η the scale parameter under use condition, α and d are the effects of ADT and corrections over η respectively. Note that we can use this simple model since there is only one ADT environment and one correction. We estimate the model parameters using numerical maximization of the log-likelihood of the failure times observed.

The reliability of the non-parametric model is calculated using Equation 5 and for the parametric model we use Equation 3.13.

$$R(t) = \exp\left(\left[\frac{t}{\hat{d}\hat{\eta}}\right]^{\hat{\beta}}\right) \tag{3.13}$$

Figure 3.6 presents the true and estimates of the reliability of the part for different life-times using both methods with the parameters listed in Table 3.1. One can see that the non-parametric model provides more accurate reliability estimates for almost every target life time, except for a small area near the intersection point of the two estimated reliability functions (roughly around 1400 hours). This result suggests that the choice of target lifetime performs a key role in which method performs better. Figure 3.7 illustrates this effect by presenting the percent relative error of

the reliability estimate at 1390 and 1400 for 100 replications of the growth program. Note that the non-parametric method presents a higher variance and lower bias than the parametric method due to the flexibility of the mean function estimate which may indicate overfitting to the small sample size.

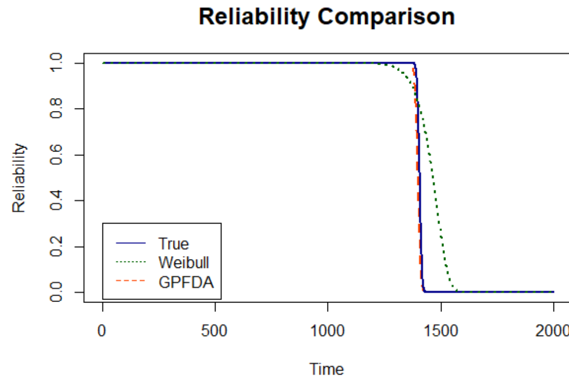

Figure 3.6: Reliability function with relatively low variance.

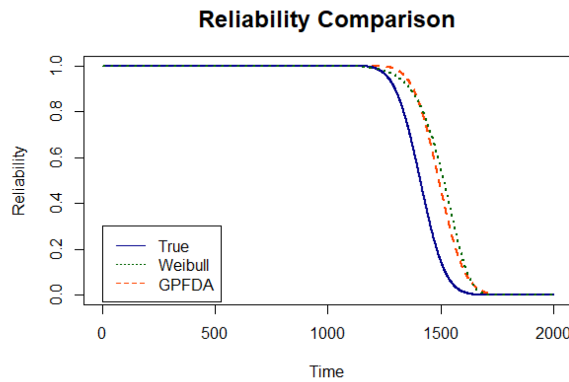

Figure 3.7: Reliability function with relatively high variance.

Lastly, Figure 3.8 presents the results of repeating the estimation process with data generated with more uncertainty such that it is harder to identify the effect of corrective actions on the degradation process. This is achieved by changing the value of λ to 0.0005 such that the variance of the IGP increases by 100 times. Both methods present a large bias for the reliability estimate, and similar results are observed even when more test units are used for each testing environment in each testing stage. This suggests that both models have trouble distinguishing the randomness

from structural changes in the underlying degradation process. In our future research, further investigation is needed to solve such problems.

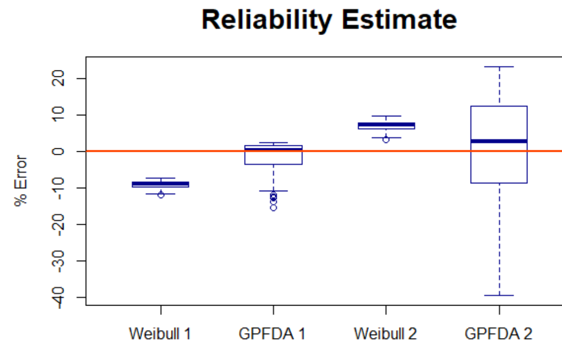

Figure 3.8: Box plot of the error on the final reliability estimate at 1390 and 1400 hours for 100 replications of the growth program.

3.5 Conclusions

In this paper, we proposed the first non-parametric methodology to model the reliability growth of a product based on its performance degradation. The product is considered failed if its performance passes a known threshold. The proposed mathematical framework estimates the reliability of the product by predicting the mean time-to-signal using FDA and capturing the unit-to-unit variation using a GP. The statistical inference procedure is capable of estimating the reliability of the product's population for any point in time, at any intermediate degradation levels, and under working conditions similar to the ones applied in the reliability growth tests.

The proposed methodology can handle monotone and non-monotone degradation processes; however, it is more efficient when the degradation process is monotone. The model can be used to predict the reliability of a product after corrective actions or the remaining useful life of a specific unit after observing the initial degradation signal of the unit. A numerical example shows that for monotone degradation processes, the non-parametric method outperforms the parametric alternatives in estimating the reliability of a unit after corrective actions have been applied. However, if the underlying noise in the degradation signal is too high, both non-parametric and parametric meth-

ods are incapable of satisfactorily identifying the changes in the degradation process introduced by corrective actions.

References

Crow, L. H. (2004). An extended reliability growth model for managing and assessing corrective actions. In *2004 Proceedings Annual Reliability and Maintainability Symposium - RAMS*, (pp. 73–80).

Hamada, M. (2005). Using degradation data to assess reliability. *Quality Engineering*, *17*(4), 615–620.

Krasich, M. (2014). Reliability growth testing, what is the real final result? Accelerated test methodology for reliability growth. In *2014 Proceedings Annual Reliability and Maintainability Symposium - RAMS*, (pp. 1–7).

Nelson, W. (1990). *Accelerated testing - statistical models, test plans, and data analysis*. John Wiley & Sons, Hoboken, New Jersey.

Shi, J. Q. & Choi, T. (2011). *Gaussian Process Regression Analysis for Functional Data*. Chapman and Hall/CRC.

Wang, X. (2010). Wiener processes with random effects for degradation data. *Journal of Multivariate Analysis*, *101*(2), 340–351.

Ye, Z.-S. & Chen, N. (2014). The Inverse Gaussian process as a degradation model. *Technometrics*, *56*(3), 302–311.

Zhou, R., Gabraeel, N., & Serban, N. (2012). Degradation modeling and monitoring of truncated degradation signals. *IIE Transactions*, *44*(9), 793–803.

4 Analysis of Correlated Multivariate Degradation Data in Accelerated Reliability Growth

Modern engineering systems have become increasingly complex and at the same time are expected to be developed faster. To shorten the product development time, organizations commonly conduct accelerated testing on a small number of units to help identify failure modes and assess reliability. Many times design changes are made to mitigate or reduce the likelihood of such failure modes. Since failure-time data is often scarce in reliability growth programs, existing statistical approaches used for predicting the reliability of a system about to enter the field are faced with significant challenges. In this work, a statistical model is proposed to utilize degradation data for system reliability prediction in an accelerated reliability growth program. The model allows the components in the system to have multiple failure modes, each associated with a monotone stochastic degradation process. To take into account unit-to-unit variation, the random effects of degradation parameters are explicitly modeled. Moreover, a mean-degradation-stress relationship is introduced to quantify the effects of different accelerating variables on the degradation processes, and a copula function is utilized to model the dependency among different degradation processes. Both a maximum likelihood (ML) procedure and a Bayesian alternative are developed for parameter estimation in a two-stage process. A numerical study illustrates the use of the proposed model and identifies the cases where the Bayesian method is preferred and where it is better to use the ML alternative.

4.1 Introduction

The competitive global business environment, fast-paced technological advancements, and increasing costumer expectations have the increased pressure to shorten product development cycles while ensuring high product reliability. In such a context, reliability growth programs and accelerated life testing (ALT) have been widely used as critical tools for meeting the business' requirements. Moreover, using prior knowledge can help speed up a reliability growth program in two ways. First, the reliability estimates may be more accurate than using maximum likelihood (ML) methods for small samples. Second, the resources for testing different subsystems of a complex system can be allo-

cated more efficiently based on the current beliefs about the system. Bayesian analysis offers a theoretical framework to incorporate previous experience with similar products and expert's judgments in product reliability prediction.

Reliability growth programs typically consists of multiple stages in which the product is tested and its design is changed to improve reliability based on the test results. This paper focuses on analyzing reliability testing data. In general, three primary types of data are collected during reliability testing: pass-fail, time-to-failure, and degradation of product performance or physical characteristics (Wilson & Fronczyk, 2017). An overview of classical Bayesian reliability models using pass-fail and time-to-failure data can be found in (Martz & Waller, 1991). In the last decades, researchers have extensively studied new models for incorporating ALT data in the Bayesian reliability growth analysis. Using pass-fail data, Strunz & Herrmann (2012) considered a Dirichlet distribution for analyzing system reliability for a rocket engine tested at extreme conditions. Using time-to-failure data, Wayne & Modarres (2015) modeled the reliability of a system with multiple failure modes subject to multiple corrections during development. Similar to Crow (2004), Wayne & Modarres (2015) modeled reliability growth was as a reduction in the failure rates of specific failure modes. Ruiz et al. (2019) considered a complex system with multiple components each having multiple failure modes and applied a simplified version of this model for reliability growth planning (Ruiz et al., 2020).

The increased availability of degradation data and improvement of computing capabilities has increased the interest on degradation-based reliability modeling in the last two decades. Failure time due to degradation is typically defined as first time that a degradation signal crosses a user defined threshold. Figure 4.1 presents an example of a monotone and a non-monotone degradation process with failure threshold of 90 and 75, respectively. Hamada (2005) showed that a Bayesian reliability model that uses degradation data may have considerably less uncertainty than its counterpart that uses time-to-failure data. This result may be explained by the extra information provided by each test unit in the form of degradation measurements and by the direct connection between the degradation process and the underlying failure mechanism. Therefore, it could be beneficial

to develop Bayesian reliability growth models based on degradation data. A comprehensive review of classical degradation models and their applications can be found in (Nelson, 1990). In the reliability literature, degradation is typically modeled as the interaction of a mean degradation function $\mu(t, x)$ of time t and covariates x, and a stochastic component. Degradation models can be classified as general path models that are based on the mean function plus measurement error ϵ or stochastic process models that are based on cumulative damage of the components. This work concentrates on the latter.

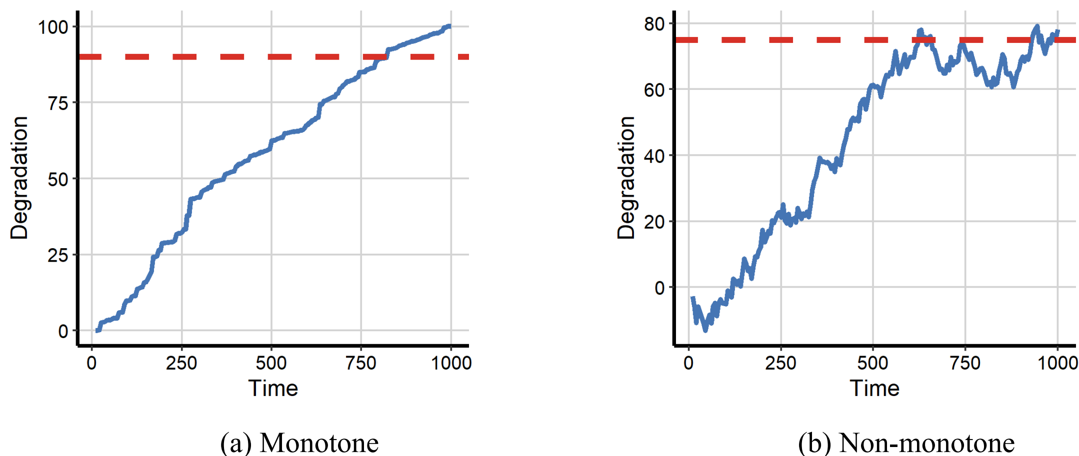

(a) Monotone (b) Non-monotone

Figure 4.1: Example of degradation signals with different failure thresholds.

The most popular stochastic degradation process models are the Wiener, Gamma, and Inverse-Gaussian (IG) processes due to their mathematical tractability and physical meaning as a random accumulation of damage (Ye & Chen, 2014). The Wiener process can be understood as adding an extra stochastic term, i.e., Brownian motion $\mathcal{B}(\cdot)$, to the General path model, and it can be expressed as $W(t) = \mu\Lambda(t) + \sigma\mathcal{B}(\Lambda(t)) + \epsilon$, where μ is the mean parameter, σ is the diffusion parameter, and $\Lambda(t)$ is a time transformation. Typically, the log-degradation signals are analyzed under this model. As an example, Liao & Elsayed (2006) used the model to predict the field reliability of a product under uncertain use conditions based on accelerated degradation testing (ADT) data. Gabraeel et al. (2005) developed a Bayesian model to predict the residual life distribution of a part under condition monitoring. In addition, Wang (2010) derived an expectation-maximization (EM) algorithm for estimating the parameters of a Wiener process with random effects.

On the other hand, the Gamma process is suitable for modeling monotone degradation processes. The key assumptions of this model is that degradation increments are independent and their magnitudes follows a Gamma distribution. Lawless & Crowder (2004) derived the closed-form expression for the probability density function (PDF) of the Gamma process when considering covariates and random effects. Ye et al. (2014) developed a semi-parametric model that incorporates a non-parametric time transformation function. However, the Gamma process is not mathematically tractable when there are measurement errors. To deal with this, Lu et al. (2013) used a mathematical transformation and quasi-Monte Carlo method for estimating the model parameters. Park & Kim (2017) used the Gamma process to analyze accelerated test data of a photo-voltaic module. They found that the Gamma process performs about the same as the linear degradation model and the Weibull life-time model in predicting the mean-time-to-failure (MTTF), but the Gamma process outperforms in the analysis of warranty data.

In the last decade, the IG process has gained popularity as an alternative to the Gamma process for modeling monotone degradation processes. Ye & Chen (2014) proved that the IG process is a limiting Poisson process and can be interpreted as a shock arrival process and used to model degradation processes with a clear physical meaning like the Gamma process. Ye & Chen (2014) also developed a maximum likelihood estimation method for cases with random effects. Peng (2015) extended this idea by developing maximum likelihood estimators with their respective confidence intervals and by incorporating explanatory variables to handle ADT data.

To the best of our knowledge, only Ruiz et al. (2019) have considered degradation for reliability growth analysis. The authors applied a non-parametric model that combines functional data analysis (FDA) and Gaussian processes (GP) for predicting the first passage time of a stochastic degradation process. However, the non-parametric method depends on testing all units to failure, and it cannot extrapolate the probability distribution of the first-passage time if a failure is redefined after changing the failure threshold. In addition, this model only considers a single failure mode in the form of a degradation process while in practice multiple degradation processes might be observed. The literature on multivariate degradation modeling is limited due to the computational

complexity of modeling correlation among processes. One approach to model such correlation is the use of multivariate Brownian motion (Sun et al., 2019), i.e., multivariate Wiener process. This approach is not suitable for monotone degradation processes. The second approach is to use copula functions to model the dependence between degradation processes (Peng et al., 2016; Wang et al., 2015; Hong et al., 2018). The drawbacks of the copula approach are that it is computationally challenging in high dimensions (Huard et al., 2006) and it is hard to incorporate physical knowledge of the correlation structure (Sun et al., 2019).

Due to the limitations of existing approaches, we propose a new parametric method to analyze accelerated reliability growth data for a component with multiple dependent degradation processes. Specially, the dependency between the increments of degradation processes is modeled using a copula function, and a parametric mean-degradation-stress relationship is introduced to quantify the effects of different accelerating variables on the degradation processes. The model parameters are estimated using either a Bayesian procedure or an ML alternative in a two-stage process. In the first stage, we estimate the parameters of multiple IG processes and the effectiveness of corrective actions throughout the reliability growth program by assuming that the degradation processes are independent. In the second stage, we fit the parameters of a copula using the estimated cumulative distribution function (CDF) of the observed degradation increments. Finally, we use the full set of parameters to predict the product's reliability for a target life under specified use conditions. This work is among the first attempts at developing a model for analyzing accelerated reliability growth data based on multiple correlated degradation processes.

The remainder of this paper is organized as follows. Section 4.2 introduces the model for the analysis of ADT data in the presence of multiple dependent degradation processes. Section 4.3 develops statistical inference methods to estimate the model parameters. Section 4.4 presents two numerical examples to illustrate the use of proposed Bayesian and ML methods. Finally, conclusions and a discussion on the contributions of this work are provided in Section 4.5.

4.2 Dependent Degradation Processes Model

This section introduces the multivariate degradation modeling approach based on copula functions, considers explanatory covariates and their effect on the degradation parameters, and discusses unit-to-unit variability of the parameters of the degradation processes.

4.2.1 Degradation Modeling

Consider a component that has N failure modes, each related to a monotonically increasing degradation process. Let $Y_i(t)$ be the degradation process i, $i = 1, ..., N$. All the degradation processes are measured at the same and multiple times t_j, and we define the degradation increment between two consecutive measurement times, t_{j-1} and t_j, as $\Delta y_{ij} = y_i(t_j) - y_i(t_{j-1})$. We assume that each degradation process can be described by an IG process, such that the PDF of degradation increments can be expressed as:

$$f(\Delta y_{ij}) = \sqrt{\frac{\lambda_i \Delta h_{ij}^2}{2\pi \Delta y_{ij}^3}} \exp\left(\frac{-\lambda_i \left[\Delta y_{ij} - \mu_i \Delta h_{ij}\right]^2}{2\Delta y_{ij} \mu_i^2}\right), \tag{4.1}$$

where μ_i and λ_i are the mean and diffusion parameters, $h_i(t)$ is a monotonic time transformation parameterized by η_i, and $\Delta h_{ij} = h_i(t_j) - h_i(t_{j-1})$.

The component is considered failed if any of the degradation processes surpasses its specific threshold $\mathcal{D}_i$. The reliability function of failure mode i at time t is given by $P\{Y_i(t) < \mathcal{D}_i\}$. For a new part with initial degradation signal equals 0 and the target life-time equals T, the reliability of process i is given by the IG cumulative CDF (Banerjee & Bhattacharyya, 1979):

$$\begin{aligned} R_i\left(\mathcal{D}_i, T|\lambda_i, \mu_i\right) = P\{Y_i(t) < \mathcal{D}_i\} =& \Phi\left(\sqrt{\frac{\lambda_i}{\mathcal{D}_i}}\left[\frac{\mathcal{D}_i}{\mu_i} - h_i\left(T\right)\right]\right) + \\ & \exp\left(2\frac{\lambda_i h_i(T)}{\mu_i}\right)\Phi\left(-\sqrt{\frac{\lambda_i}{\mathcal{D}_i}}\left[\frac{\mathcal{D}_i}{\mu_i} + h_i\left(T\right)\right]\right). \end{aligned} \tag{4.2}$$

The stochastic dependence between the degradation increments of the multiple processes is modeled using a copula function (Peng et al., 2016; Hong et al., 2018; Wang et al., 2015). A copula is a multivariate function defined over a $[0, 1]$ hypercube of any dimensionality. In addition, any continuous multivariate distribution can be expressed in terms of a copula function $C(\cdot)$ and the marginal CDFs of its dimensions (dos Santos Silva & Lopes, 2008). Thus, the component's reliability at the target life-time T given a vector of degradation threshold $\mathcal{D} = [\mathcal{D}_1, \ldots, \mathcal{D}_N]$ is:

$$R(T|D^f) = P\left\{Y_1(T) < \mathcal{D}_1 \cdots, Y_N(T) < \mathcal{D}_N\right\} = C\left(R_1\left(\mathcal{D}_1, T\right), \cdots, R_N\left(\mathcal{D}_N, T\right)\right). \quad (4.3)$$

The use of copula models introduces the difficulty of selecting an appropriate copula function $C(\cdot)$ to capture the correlation among processes. Common choices of $C(\cdot)$ are the Archimedean and Gaussian copulas (Huard et al., 2006; dos Santos Silva & Lopes, 2008) due to their numerical tractability in low dimensions. Another approach is the use of non-parametric functions based on kernel basis (Chen & Huang, 2007). We discuss how to select the copula function in Section 4.3.3.

4.2.2 Explanatory Variables

The effects of stresses (i.e., accelerating variables) on different degradation processes are captured by the stress-dependent inverse-mean parameters. We assume that there are L accelerating variables such that the mean degradation parameter of degradation process i can be expressed as:

$$\mu_i(x) = \mu_{0i} \exp\left(\sum_{\ell=1}^{L} \theta_{\ell i} x_\ell\right), \quad (4.4)$$

where μ_{0i} is the baseline mean degradation parameter (i.e., under use condition), and x_ℓ is the normalized stress level for the ℓth stressor. The normalization used is of the form $x = {(z - z^-)}/{(z^+ - z^-)}$ where z^- and z^+ are the minimum and maximum levels of the stressor that does not change the underlying failure mechanism of the degradation process. This parameterization implies that $0 \leq x_\ell \leq 1$, and $\theta_{\ell i} \geq 0$ in order to observe a higher degradation rate during accelerated testing. Note that this is a common choice of parameterization (Ye & Chen, 2014) and it is equivalent to

the Arrhenius model by transforming the stress level as $z = \zeta^{-1}$ and to the power law model by transforming the stress level to $z = \ln(\zeta)$, where ζ is the original stress value. Lastly, the reliability of the component can still be calculated using Equation (4.2) by replacing μ_i with $\mu_i(x)$.

4.2.3 Random Effects

The base model is the one with no random effects (NRE) as discussed in Section 4.2.1. We propose two approaches for modeling unit-to-unit variation on the parameters of the degradation processes. First, random effects on the inverse-mean (REM) are incorporated by assuming that $m_{0i} = \mu_{0i}^{-1}$ follows a Truncated Normal distribution with mean ν_i and dispersion $\tau_i = \sigma^{-2}$ with the minimum value of 0. This implies that the PDF of the inverse-mean has a regularizing constant $\Phi'(\cdot) = 1 - \Phi(\cdot)$ where $\Phi(\cdot)$ is the CDF of the standard Normal distribution. After integrating out m_{0i}, the PDF of the vector of degradation increments $\Delta\mathbf{y}_{ik} = (\Delta y_{i1k}, \Delta y_{i2k}, \ldots, \Delta y_{in_k k})$ for unit k is:

$$f\left(\Delta\mathbf{y}_{ik}\right) = \frac{1}{\Phi'(-\nu_i\sqrt{\tau_i})} \prod_{j=1}^{n_k} \sqrt{\frac{\lambda_i \Delta h_{ijk}^2}{2\pi\Delta y_{ijk}^3}} \sqrt{\frac{\tau_i}{\lambda_i Y_{ik}\mu_{xik}^2 + \tau_i}} \exp\left(\frac{-\gamma}{2}\right) \Phi'\left(\frac{-\lambda_i\mu_{xik}H_{ik} - \nu_i\tau_i}{\sqrt{\lambda_i Y_{ik}\mu_{xik}^2 + \tau_i}}\right), \tag{4.5}$$

where

$$\mu_{xik} = \exp\left(-\sum_{\ell=1}^{L} \theta_{\ell i} x_\ell\right), \qquad Y_{ik} = \sum_{j=1}^{n_k} \Delta y_{ijk},$$

$$H_{ik} = \sum_{j=1}^{n_k} \Delta h_{ijk}, \qquad HY_{ik} = \sum_{j=1}^{n_k} \frac{\Delta h_{ijk}^2}{\Delta y_{ijk}},$$

$$\gamma = \left[\lambda_i HY_{ik} + \tau_i\nu_i^2 - \frac{(\lambda_i\mu_{xik}H_{ik} + \nu_i\tau_i)^2}{\lambda_i Y_{ik}\mu_{xik}^2 + \tau_i}\right].$$

It is worth pointing out that there is no closed-form expression for the reliability function of failure mode i under this model, thus a numerical method is needed for evaluating the following integral:

$$R_i(T|x) = \int_0^{\mathcal{D}_i} \frac{1}{\Phi'(-\nu_i\sqrt{\tau_i})}\sqrt{\frac{\lambda_i h(T)^2}{2\pi\Delta y^3}}\sqrt{\frac{\tau_i}{\lambda_i y\mu_{xi}^2+\tau_i}}\exp\left(\frac{-\gamma_i}{2}\right)\Phi'\left(\frac{-\lambda_i h(T)\mu_{xi}-\nu_i\tau_i}{\sqrt{\lambda_i y\mu_{xi}^2+\tau_i}}\right)dy, \tag{4.6}$$

where

$$\gamma_i = \tau_i\nu_i^2 + \lambda_i\frac{h(T)^2}{y} - \frac{(\lambda_i h(T)\mu_{xi}+\nu_i\tau_i)^2}{\lambda_i y\mu_{xi}^2+\tau_i}.$$

The second model incorporates random effects for both degradation parameters (REB). The joint distribution of (m_{0i}, λ_i) is assumed to be a Truncated Normal-Gamma with PDF:

$$g(\lambda_i, m_i) = \frac{\beta_i^{\alpha_i}}{\Gamma(\alpha_i)}\lambda_i^{\alpha_i-1}\exp(-\beta_i\lambda_i)\sqrt{\frac{\lambda_i\tau_i}{2\pi}}\exp\left(-\frac{\lambda_i\tau_i(m_i-\nu_i)^2}{2}\right)\frac{1}{\Upsilon'_{2\alpha_i}(-\nu_i\sqrt{\tau_i\alpha_i/\beta_i})}, \tag{4.7}$$

where $\Upsilon'_q = 1 - \Upsilon_q$, and Υ_q is the standard Student's t-distribution with q degrees of freedom.

Similar to the first model, the PDF of degradation increments under the REB model can be expressed as:

$$\begin{aligned} f(\Delta\mathbf{y}_{ik}) = \prod_{j=1}^{n_k}\left[\sqrt{\frac{\Delta h_{ijk}^2}{2\pi\Delta y_{ijk}^3}}\right]\frac{1}{\Upsilon'_{2\alpha_i}(-\nu_i\sqrt{\tau_i\alpha_i/\beta_i})}\frac{\beta_i^{\alpha_i}}{\Gamma(\alpha_i)}\sqrt{\frac{\tau_i}{Y_{ik}\mu_{xik}^2+\tau_i}}\frac{\Gamma(\alpha_i+n_k/2)}{\omega_{ik}^{\alpha_i+n_k/2}} \\ \times\Upsilon'_{2\alpha_i+n_k}\left(-[\mu_{xik}H_{ik}+\nu_i\tau_i]\sqrt{\frac{2\alpha_i+n_k}{2(Y_{ik}\mu_{xik}^2+\tau_i)\omega_{ik}}}\right), \end{aligned} \tag{4.8}$$

where

$$\omega_{ik} = \beta_i + \frac{1}{2}\left[HY_{ik} + \tau_i\nu_i^2 - \frac{(\mu_{xik}H_{ik}+\nu_i\tau_i)^2}{Y_{ik}\mu_{xik}^2+\tau_i}\right].$$

Moreover, the reliability function of each failure mode under this model can be calculated by

evaluating the following integral:

$$R_i(T|x) = \int_0^{\mathcal{D}_i} \sqrt{\frac{h_i(T)^2}{2\pi\Delta y^3}} \frac{1}{\Upsilon'_{2\alpha_i}(-\nu_i\sqrt{\tau_i\alpha_i/\beta_i})} \frac{\beta_i^{\alpha_i}}{\Gamma(\alpha_i)} \sqrt{\frac{\tau_i}{y\mu_{xik}^2+\tau_i}} \frac{\Gamma(\alpha_i+1/2)}{\omega_i^{\alpha_i+1/2}} \times \Upsilon'_{2\alpha_i+1}\left(-\left[\mu_{xik}h_i(T)+\nu_i\tau_i\right]\sqrt{\frac{2\alpha_i+1}{2(y\mu_{xik}^2+\tau_i)\omega_i}}\right) dy, \tag{4.9}$$

where

$$\omega_i = \beta_i + \frac{1}{2}\left[\tau_i\nu_i^2 + \frac{h_i(T)^2}{y} - \frac{(h_i(T)\mu_{xik}+\nu_i\tau_i)^2}{y\mu_{xik}^2+\tau_i}\right].$$

4.2.4 Reliability Growth Program

The reliability growth program consists of S test-fix stages with corrective actions (i.e., design changes) at the end of each stage. Corrections may reduce the mean degradation, the dispersion parameter, or both for a degradation process. The effects of corrective actions are modeled as changes in the parameters such that during stage s, we have:

$$\nu_{is} = \nu_i \prod_{s'=1}^{s-1} d_{\nu_i s'} \qquad \tau_{is} = \tau_i \prod_{s'=1}^{s-1} d_{\tau_i s'} \qquad \theta_{\ell is} = \theta_{\ell i} \prod_{s'=1}^{s-1} d_{\theta_{\ell i} s'} \qquad \beta_{is} = \beta_i \prod_{s'=1}^{s-1} d_{\beta_i s'},$$

where $d_{\nu_i s}$ is the effectiveness of correction s over ν, $d_{\tau_i s}$ is the one over τ, $d_{\theta_{\ell i} s}$ is the one over θ_ℓ, and $d_{\beta_i s}$ is the one over β. Corrective actions improve the reliability if:

- $d_{\nu_i s} > 1$, such that ν_i increases as the mean degradation ν_i^{-1} decreases.
- $d_{\tau_i, s} > 1$, such that units become more consistent and the product has better quality. Note that this implies a change in the shape of the reliability function such that more units fail around their MTTF. In other words, the reliability calculated at time before the MTTF will increase while it will decrease at time after the MTTF.
- For the NRE model, μ_i is fixed and the improvement would mean a reduction on the mean parameter. Therefore, we consider $\mu_{is} = \mu_i \prod_{s'=1}^{s-1} d_{\nu_i s'}^{-1}$.

- $d_{\theta_{\ell i}s} < 1$, such that the mean degradation is less sensitive to the environmental factors.
- $d_{\beta_i s} < 1$, such that the variation of degradation increments is reduced. The component has a better quality and lower population reliability by the same logic as for the changes on τ_i. Note that corrective actions on λ_i are only captured on β_i which reflects the effect of multiplying the distribution of λ_i by a constant, whereas, changing α_i does not have a clear meaning. Therefore, $\lambda_{is} = \lambda_i \prod_{s'=1}^{s-1} d_{\beta_i s'}^{-1}$ for the NRE and REM models.

Lastly, parameters β_i and α_i tend to ∞ when there are no significant random effects on λ. Similarly, τ tends to ∞ when m_{0i} is the same for all units. Therefore, if the MLEs of these parameters are significantly large, this shows a strong indication that the random effects are not significant enough to be considered in the model. Ye & Chen (2014) presented a hypothesis test procedure based on this idea for testing the significance of random effects when the degradation process is well described by a Gamma process. However, there is no obvious counterpart for the IG process under reliability growth, since the random effects may be significant in the early designs or may be introduced in later design changes.

4.3 Parameter Estimation

It is assumed that during each test-fix stage s of the reliability growth program, P_s testing environments are used, κ_{ps} units are tested under environment p at stage s, and n_{kps} degradation measurements are taken for unit k. Without loss of generality, we assume that the reliability growth program must be completed before time $\mathcal{T}$, and measurements are taken on all degradation processes simultaneously (i.e., there is no missing information).

Let Λ be the data composed of stage s, stress environment x_{ps}, unit number k, degradation measurement y_{ijkps}, and measurement time t_{jkps}. The full likelihood function of all model parameters

Θ can be expressed as:

$$\mathcal{L}(\Theta|\Lambda) = \prod_{s=1}^{S}\prod_{p=1}^{P_s}\prod_{k=1}^{\kappa_{ps}}\prod_{j=1}^{n_{kps}} C\left(R_1(y_{1jksp}, t_{jkps}), \ldots, R_N(y_{1jksp}, t_{jkps})|\Theta\right). \tag{4.10}$$

It is worth pointing out that Equation (4.10) or its natural logarithm (i.e., log-likelihood) are far too complex to solve analytically for any common choice of copula function. To fit the model parameters, a common approach is to use a two-stage process (Wang et al., 2015; Peng et al., 2016). The first stage consists of fitting the parameters of the degradation processes as if these degradation processes were independent. The second stage is focused on fitting the parameters of the copula function based on the estimated CDFs of the observed degradation increments.

Next, both an ML procedure and a Bayesian alternative for the first stage are provided, and the selection of copula function in the second stage based on these two estimation methods is also examined.

4.3.1 MLE Procedure

In the context of MLEs, the first step can be done by maximizing the log-likelihood function of each degradation process as if they were independent using a numerical maximization algorithm. In order to get the log-likelihood function of the data under the different models, we first define:

$$Y_{ikps} = \sum_{j=1}^{n_{kps}} \Delta y_{ijkps}, \qquad H_{ikps} = \sum_{j=1}^{n_{kps}} \Delta h_{ijkps}, \qquad HY_{ikps} = \sum_{j=1}^{n_{kps}} \frac{\Delta h_{ijkps}^2}{\Delta y_{ijkps}}.$$

In addition, let Θ_i be the set of parameters for degradation process i and Λ_i be the data related to this process observed during the reliability growth program. Then, the log-likelihood of the NRE model can be expressed as:

$$\ln\left(\mathcal{L}\left(\Theta_i|\Lambda_i\right)\right) \propto \sum_{s=1}^{S}\sum_{p=1}^{P_s}\sum_{k=1}^{\kappa_{ps}}\sum_{j=1}^{n_{kps}} \frac{\ln(\lambda_{is})}{2} + \ln\left(\Delta h_{ijkps}\right)$$

$$
- \frac{\lambda_{is}\mu_{xips}^2}{2\mu_{is}^2 \Delta y_{ijkps}^2} \left(\Delta y_{ijkps} - \frac{\mu_{is}}{\mu_{xips}} \Delta h_{ijkps} \right)^2 . \tag{4.11}
$$

The log-likelihood function of the parameters of REM model can be expressed as:

$$
\begin{aligned}
\ln\left(\mathcal{L}\left(\Theta_i|\Lambda_i\right)\right) \propto \sum_{s=1}^{S}\sum_{p=1}^{P_s}\sum_{k=1}^{\kappa_{ps}} \Bigg[& \frac{n_{kps}}{2}\ln\left(\lambda_{is}\right) + \frac{\ln(\tau_{is})}{2} - \frac{1}{2}\ln\left(\lambda_{is}Y_{ikps}\mu_{xips}^2 + \tau_{is}\right) \\
& + \sum_{j=1}^{n_{kps}} \ln\left(\Delta h_{ijkps}\right) - \frac{1}{2}\left[\lambda_{is} HY_{ikps} + \tau_{is}\nu_{is}^2 - \frac{\left(\lambda_{is}\mu_{xips}H_{ikps} + \nu_{is}\tau_{is}\right)^2}{\lambda_{is}Y_{ikps}\mu_{xips}^2 + \tau_{is}}\right] \\
& + \ln\left\{\Phi'\left(\frac{-\lambda_{is}\mu_{xips}H_{ikps} - \nu_{is}\tau_{is}}{\sqrt{\lambda_{is}Y_{ikps}\mu_{xips}^2 + \tau_{is}}}\right)\right\} - \ln(\Phi'(-\nu_{is}\sqrt{\tau_{is}}))\Bigg].
\end{aligned} \tag{4.12}
$$

Similarly, the log-likelihood function of the REB model is:

$$
\begin{aligned}
\ln\left(\mathcal{L}(\Theta_i|\Lambda_i)\right) \propto \sum_{s=1}^{S}\sum_{p=1}^{P_s}\sum_{k=1}^{\kappa_{ps}} \Bigg[& \alpha_i \ln\left(\beta_{is}\right) - \ln\left(\Gamma(\alpha_i)\right) - \ln\left(\Upsilon'_{2\alpha_i}(-\nu_{is}\sqrt{\tau_{is}\alpha_{is}/\beta_{is}})\right) + \sum_{j=1}^{n_{kps}} \ln(\Delta h_{ijkps}) \\
& - \frac{1}{2}\ln(Y_{ikps}\mu_{xips}^2 + \tau_{is}) + \ln\left[\Gamma\left(\alpha_i + \frac{n_{kps}}{2}\right)\right] - \left(\alpha_i + \frac{n_k}{2}\right)\ln(\omega_{ikps}) + \frac{\ln(\tau_{is})}{2} \\
& + \ln\left\{\Upsilon'_{2\alpha_i+n_k}\left(-\left[\mu_{xips}H_{ikps} + \nu_{is}\tau_{is}\right]\sqrt{\frac{2\alpha_i + n_{kps}}{2(Y_{ikps}\mu_{xips}^2 + \tau_{is})\omega_{ikps}}}\right)\right\}\Bigg],
\end{aligned} \tag{4.13}
$$

where

$$
\omega_{ikps} = \beta_{is} + \frac{1}{2}\left[HY_{ikps} + \tau_{is}\nu_{is}^2 - \frac{\left(\mu_{xips}H_{ikps} + \nu_{is}\tau_{is}\right)^2}{Y_{ikps}\mu_{xips}^2 + \tau_{is}}\right].
$$

For the second step, the CDF of the observed degradation increments is calculated using Equation 4.2 and the MLEs of the parameters of the degradation process for each unit, which are calculated as follows:

$$
\hat{m}_{ikps} = \hat{m}_{0ikps}\mu_{xips} = \frac{\hat{H}_{ikps}}{Y_{ikps}} \tag{4.14}
$$

$$
\hat{\lambda}_{ikps} = n_{ikps}\left[\hat{HY}_{ikps} - \frac{\hat{H}_{ikps}^2}{Y_{ikps}}\right] \tag{4.15}
$$

where $\hat{H}$ and $\hat{HY}$ are calculated based on the estimated parameter of $h(\cdot)$, $\hat{\mu}_{ik}$ is calculated when assuming either the REM or REB model and $\hat{\lambda}_{ik}$ is calculated when assuming the REB model, Note that for the NRE model we already have the MLEs of all parameters. Lastly, the parameters of any given copula function can be estimated via maximum likelihood using specialized software packages available in R such as VineCopula (Schepsmeier et al., 2018).

4.3.2 Bayesian Procedure

For the first stage under the Bayesian framework, the posterior distribution of the parameters of the degradation process is sampled using a sequential Metropolis-Hasting (MH) algorithm (Hamada et al., 2008). The idea is to sample the posterior distribution of each parameter one at a time using a one dimensional MH algorithm given the current sample of all the other parameters. Algorithm 3 describes the sampling process for each parameter. Note that the posterior of the parameters can be sampled in any order, use any proposal distribution, and any posterior distribution without changing the inference of the model parameters once the sample has converged to its posterior distribution. However, the speed of convergence of the sampled parameters to their posterior distribution depends on the choice of parameters for the MH algorithm. The log-likelihood functions for the NRE, REM, and REB models are Equations (4.11), (4.12), and (4.13), respectively.

Algorithm 3 MH algorithm

Require: Proposal distribution $q(\cdot)$, prior distribution $\pi(\cdot)$, and initial value θ_c

1: Sample proposed value θ_p from $q(\theta|\theta_c)$ and u from Uniform$(0, 1)$

2: **if** $\frac{q(\theta_c|\theta_p)}{q(\theta_p|\theta_c)} \frac{\mathcal{L}(\theta_p|\Theta \notin \theta, \boldsymbol{t})\pi(\theta_p|\Omega_\theta)}{\mathcal{L}(\theta_c|\Theta \notin \theta, \boldsymbol{t})\pi(\theta_c|\Omega_\theta)} \leq u$ **then**

3: Accept θ_p and return it

4: **else**

5: Reject θ_p and return θ_c

In the second stage, the mean values (medians are another option) of the posterior samples are used as the hyperparameters of the prior distribution of the parameters of the degradation process for each unit, and the mean value of the parameters of $h(\cdot)$ is used as its point estimate. The priors are the Normal and Normal-Gamma distribution for the REM and REB model, respectively. Then,

we obtain the posterior parameters for each unit under the REB model by using the following equations:

$$
\begin{aligned}
\tau_{ikps} &= \bar{\tau}_{is} + Y_{ikps}, \\
\mu_{ikps} &= \frac{\bar{\tau}_{is}\bar{\mu}_{is}\bar{\upsilon}_{ips} + \hat{H}_{ikps}}{\tau_{ikps}}, \\
\beta_{ikps} &= \bar{\beta}_{is} + \frac{\bar{\tau}_{is}\bar{\mu}_{is}^2\bar{\upsilon}_{ips}^2}{2} + \frac{\hat{HY}_{ikps}}{2} - \frac{\tau_{ikps}\mu_{ikps}^2}{2}, \\
\alpha_{ikps} &= \bar{\alpha}_{is} + \frac{n_k}{2}.
\end{aligned}
$$

For the REM model, τ_{ikps} is calculated the same way, and

$$
\mu_{ikps} = \frac{\bar{\tau}_{is}\bar{\mu}_{is}\bar{\upsilon}_{ips} + \bar{\lambda}_{is}\hat{H}_{ikps}}{\tau_{ikps}}.
$$

For both models, we use the expected value of the posterior distribution as point estimates of the parameters of the degradation process for each unit to estimate the CDFs of the observed degradation increments. Lastly, the posterior distribution of the parameters of the copula function can be sampled using a standard Metropolis-Hasting algorithm, and the log-likelihood functions for the most commonly used copula functions can be found in (Huard et al., 2006).

4.3.3 Copula Selection

The copula function is selected using the Bayesian information criteria (BIC) for the ML procedure and the Expected BIC (EBIC) for the Bayesian procedure (dos Santos Silva & Lopes, 2008). The respective criteria are:

$$
\text{BIC}(\hat{\Theta}_c|C,\Lambda) = -2\ln\left(\mathcal{L}(\hat{\Theta}_c, C|\Lambda)\right) + \ln(n)K_c, \tag{4.16}
$$

$$
\text{EBIC}(\Theta_c|C,\Lambda) = -\frac{2}{M}\sum_{i=1}^{M}\ln\left(\mathcal{L}(\Theta_{ci}, C|\Lambda)\right) + \ln(n)K_c, \tag{4.17}
$$

where C is the copula function, Θ_c consists of the parameters of C, K_c is the number of parameters for C, $\hat{\Theta}_c$ is the MLE of the parameters, n is the total number of degradation measurements, M is the number of posterior samples, and Θ_{ci} is the ith posterior sample of the parameters. The properties of commonly used copula functions and the domains of their parameters based on Kendall's τ (measure of the rank correlation between random variables) can be found in (Huard et al., 2006). We consider the Clayton, Gaussian, and Gumbel copulas for model selection as they can capture different correlation structures. As shown in Figure 4.2, the Clayton copulas have stronger correlation in the lower quantiles, the Gaussian copulas present the same correlation across all quantiles, and the Gumbel copulas have stronger correlation at higher quantiles.

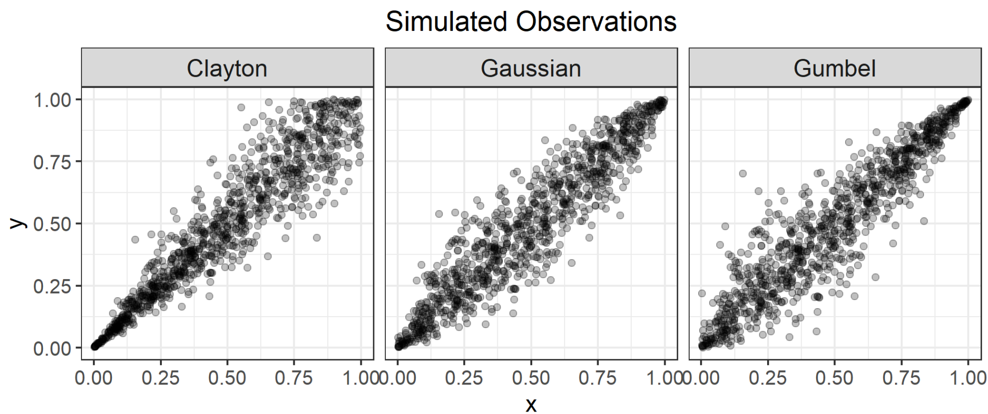

Figure 4.2: Pairs of random variables under different copula functions.

4.4 Numerical Example

In this section, two numerical examples are provided to illustrate the effectiveness of the proposed methodology. The first example explores the reliability prediction capabilities of the proposed methods when the true degradation processes present random effects on both the inverse-mean and diffusion parameters, only the mean parameter, or neither parameter. The second example studies the properties of both ML and Bayesian methods for cases with multiple replications of a reliability growth program.

4.4.1 System Description

The example simulates a two-stage reliability growth program for a system with two failure modes. The system is sensitive to one stress factor of interest, and the highest stress level is $x = 1$. In the each stage, 3 units are tested at the use condition and 3 more at the highest stress level (i.e., $x = 0$ and $x = 1$, respectively). The total testing time for all units is 100 hours, and degradation measurements are taken every four hours such that a total of 25 measurements are taken from each unit if it does not fail. One correction is applied at the end of the first text-fix stage, and its effect is estimated based on the testing results at the end of the second stage. We use a power-law time transformation for $h(t) = t^{\eta}$.

Table 4.1: Parameters of each degradation process when there are radom effects on (m_{0i}, λ_i).

Failure Mode	$\mathcal{D}$	ν_i	τ_i	θ_i	α_i	β_i	η_i	$d_{\nu_i s}$	$d_{\tau_i s}$	$d_{\theta_i s}$	$d_{\beta_i s}$
1	100	10	1.0	0.51	2	10	1.10	1.20	1.5	0.70	0.77
2	100	12	0.8	0.54	2	12	1.11	1.18	2.0	0.71	0.91

The parameters of the degradation processes are shown in Table 4.1. Note that under these parameters, units rarely fail when tested at the use condition for less than 200 hours. The Clayton copula function with Kendall's $\tau = 0.5$ is used to generate the degradation increments. For the implementation of the Bayesian method, all the numerical examples use chains with $100,000$ samples. In addition, neither burn-in nor thinning is applied to the chains because we are only interested in calculating the point estimates of model parameters of each degradation process. Otherwise, the length of the chains must be increased drastically due to the high auto correlation between consecutive sample draws of the posterior distribution. Table 4.2 presents the order in which the parameters are sampled for the REB model. The same order is followed for the REM model with the difference that λ_i is sampled instead of α_i and β_i. Table 4.2 also shows the prior distribution used for the model parameters. Since all model parameters must be non negative, the priors used are the Truncated Normal $\mathcal{TN}$ and Gamma $\mathcal{G}$ distributions. The hyperparameters of the priors are set such that the prior has the expected value equal to the true value of the parameter and the variances equal

to 1. The proposal distribution for all the parameters is the Truncated Normal with the mean being the current sample of the parameter and the standard deviation being fixed at 0.25. In addition, the prior distribution of the copula parameters is induced through Kendall's τ. We started with a uniform distribution between the minimum and maximum values of Kendall's τ for each copula function and then made a change of variables to obtain the prior distribution of its parameters. The equations for this relationship can be found in (Huard et al., 2006).

Table 4.2: Characteristics of the sequential MH procedure.

Parameter	ν_i	$d_{\nu_i s}$	θ_i	$d_{\theta_i s}$	τ_i	$d_{\tau_i s}$	α_i	β_i	$d_{\beta_i s}$	η_i
Order	1	2	3	4	5	6	7	8	9	10
Prior	$\mathcal{TN}$	$\mathcal{TN}$	$\mathcal{TN}$	$\mathcal{TN}$	$\mathcal{G}$	$\mathcal{G}$	$\mathcal{G}$	$\mathcal{G}$	$\mathcal{G}$	$\mathcal{TN}$

4.4.2 Reliability Prediction

In this section, reliability functions are presented for both parameter estimation methodologies assuming no random effects (maximum likelihood estimate-MLE and Bayesian estimate-BE), random effects on the inverse-mean (MLEM and BEM), and random effects on both the inverse-mean and diffusion parameters (MLEB and BEB), In addition, the Bayesian methods use informative priors (i.e. variance equals 1).

Figure 4.3 shows the reliability functions estimated when the true model is REB. The estimated functions intercept roughly around 700 hours since all methods result in biased estimates of the location (ν_i) of the inverse-mean parameters. On the other hand, the shapes of the BEB and MLEB are similar to that of the true reliability function while the reliability functions obtained from the other methods drop much faster. This result is expected due to the small number of units tested which do not provide enough information on the degradation rate whereas η, α, and β are estimated more accurately with 300 observed degradation increments.

Figure 4.4 presents the same study when the true model is either REM or NRE. The data for REM was generated by using the shape parameter as the expected value of the distribution used for REB (i.e., $\lambda_i = \alpha_i/\beta_i$), and for NRE we also defined the inverse-mean as the expected value of this

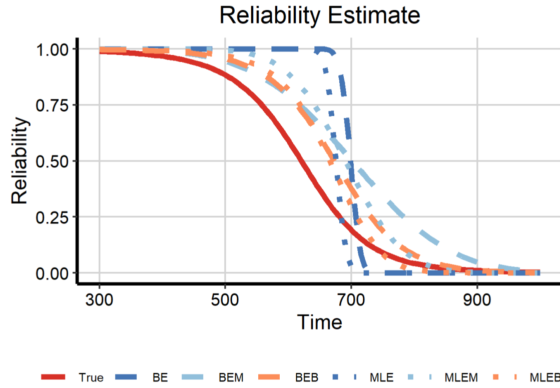

Figure 4.3: Estimated reliability curves when 3 units are tested for 100 hours in each condition and the true model presents random effects on both parameters.

parameter in REB (i.e., $m_{0i} = \nu_i$). Figure 4.4b shows that when no random effects are present, the estimated reliability function is very close to the true value even with only 3 units tested. This is due to the reduction on the uncertainties in the true system and the flexibility of the REM and REB methodologies to increase the estimated τ_i to account for the low variability in the inverse-mean parameter, and increase α_i and β_i in a similar proportion to maintain a stable expected value of λ_i while reducing its uncertainty. On the other hand, Figure 4.4a shows that the models still show a significant bias on the inverse-mean estimate when the true model is REM. This is expected since more units are needed to estimate the inverse-mean parameter under REM than under NRE.

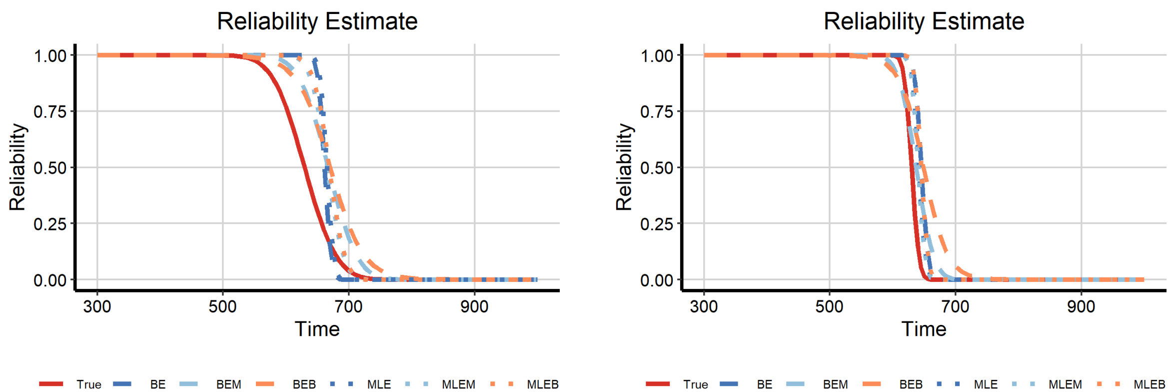

(a) True model: REM

(b) True model: NRE

Figure 4.4: Estimated reliability functions with different true models.

Figure 4.5 presents the effect of either duplicating the number of measurements (by increasing

the inspection frequency) or the number of units tested. Figure 4.5a shows that increasing the number of measurements improves the shape of the reliability funtion while reducing the bias on the inverse-mean parameter. This effect is not observed for BE and MLE since not much new information is gained by increasing the number of measurements when there are no random effects. On the other hand, Figure 4.5b shows that increasing the number of units significantly improves the final estimate. Note that this should be the case since not only more units are observed, but the effective number of degradation measurements also doubles.

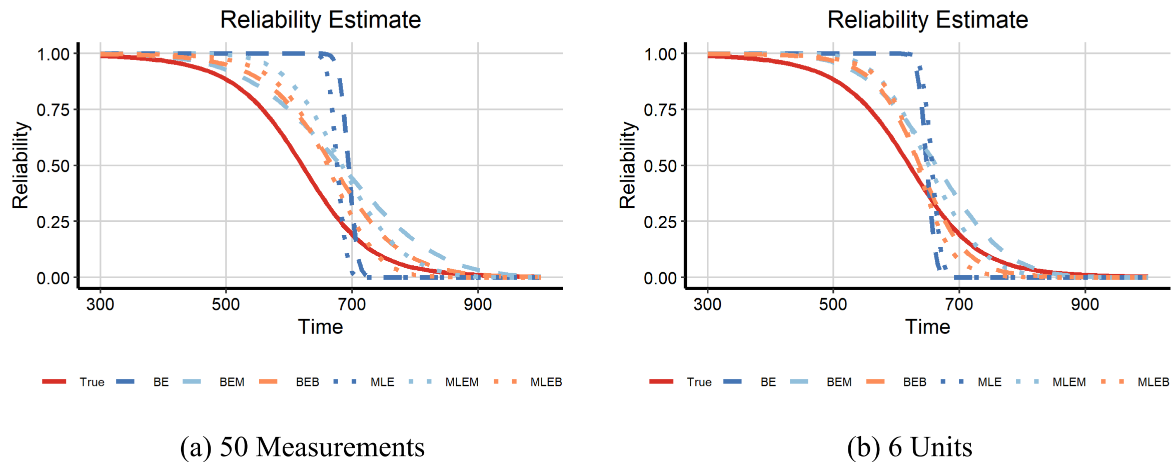

(a) 50 Measurements

(b) 6 Units

Figure 4.5: Estimated reliability curves when either the number of measurements or the number of units increases.

4.4.3 Performance with Multiple Replications

We compare the performance of the Bayesian and ML methodologies based on 100 replications of the reliability growth program when the true model is REB. The Bayesian method use informative priors with variance equals 1 (Bay) or relatively uninformative (flat) priors with variance equals 100 (BayF). The program has three test settings with different numbers of measurements and units tested in each condition. The base case has 25 measurements and 3 units: (25,3), the second has 50 measurements and 3 units: (50,3), and the last one tests 6 units with 25 measurements: (25,6). In addition, we also fit both the REB and NRE models. The results are compared in terms of relative

error of the parameter estimate $\hat{\theta}$ against the true parameter $\tilde{\theta}$ as:

$$re = \frac{\hat{\theta} - \tilde{\theta}}{\tilde{\theta}}. \tag{4.18}$$

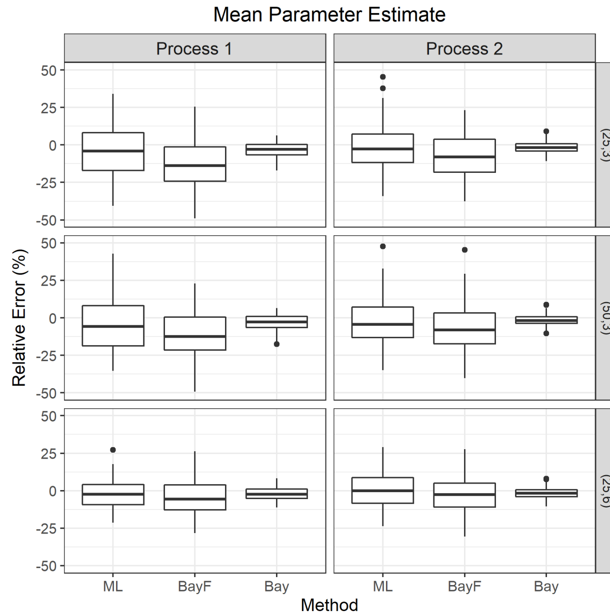

Figure 4.6: Relative error of the mean inverse-degradation (ν) estimate.

Figure 4.6 shows the relative error of the estimate of the inverse-mean parameter ν_i. Note that the reliability function and MTTF of the system are sensitive to this parameter. The ML methods present higher variances on their point estimates than the Bayesian methods and a slight bias to a lower estimate (i.e., higher mean degradation). Increasing the number of measurements reduces the variability of the estimates without reducing the bias. As expected, increasing the number of units decreases both the bias and variance of the estimates using both Bayesian and ML methods.

Figure 4.7 compares the NRE and REB models on their estimates of the MTTF of the system after corrections. For both Bayesian and ML methods, the NRE model presents a higher variance and bias than the REB model. This result indicates that using a simpler model can lead to significant errors even for estimating the MTTF of the system. For the REB model, the flat priors result in worse performance that using the MLE which might be due to requiring more samples to converge

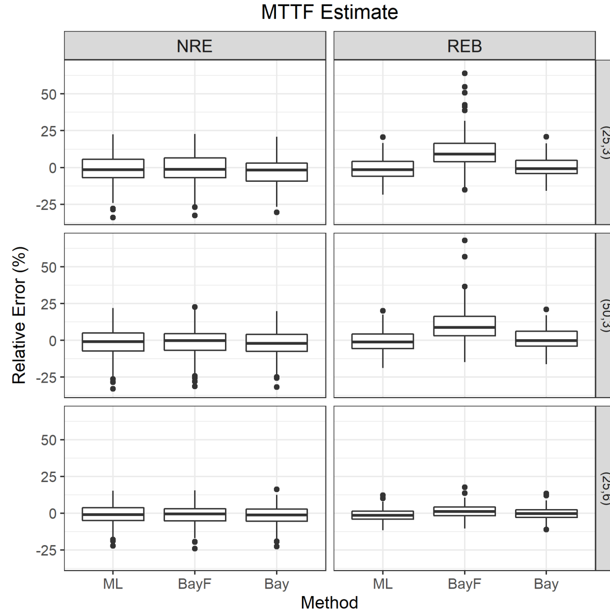

Figure 4.7: Relative error of the MTTF estimate.

to the posterior distribution. On the other hand, the estimates based on informative priors present a slightly less bias than the ML estimates while having roughly the same variability. This result seems to contradict with the results in Figure 4.6 since one would expect to observe a similar behavior on both figures. This apparent contradiction can be explained by examining the estimate of the final mean of the inverse-mean parameter (see Figure 4.8). The variability of the estimate of the improved (corrected) mean of the inverse-mean degradation is similar for both informative Bayesian and ML methods, while being worse for the Bayesian with flat priors. The main difference is that the informative Bayesian method presents a negative bias when only 3 units are tested, specially for process 2. This result indicates that the informative Bayesian method assigns all the uncertainty to the estimate of the correction factor d_{ν_s} while keeping the estimate of ν close to its initial value. In practical terms, both methods have a similar performance in predicting the MTTF but can present significantly different conclusions on the observed reliability growth (i.e., the estimate of d_{ν_s}).

Lastly, we study the ability of the methodologies to select the correct copula function and estimating its parameter. Table 4.3 presents the proportion of replications that the BIC or EBIC leads to

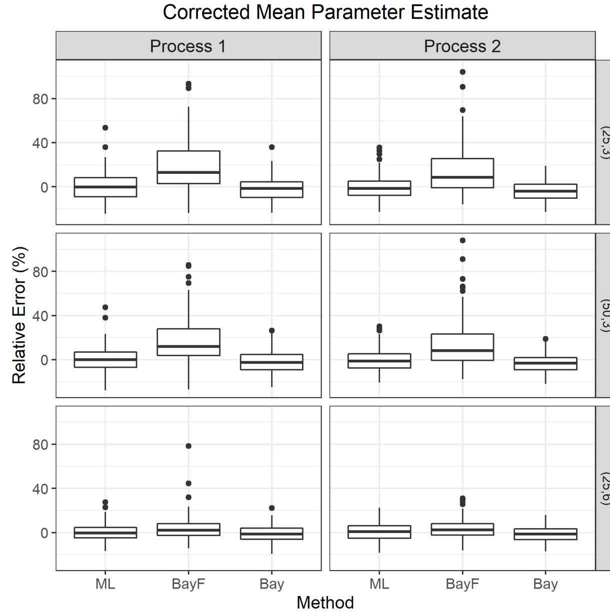

Figure 4.8: Relative error of the corrected mean inverse-degradation (νd_{ν_s}) estimate.

selecting the correct copula function for both NRE and REB models. Ignoring the random effects can lead to choosing the wrong copula function. In particular, the ML method struggles to select the correct copula even under the REB model. On the other hand, the Bayesian method is robust to errors on the parameter estimates of the degradation processes since the proportion of correct selection ir high regardless of the prior and model. Increasing the number of measurements improves the chance for correct selection while increasing the the number of units makes the selection worse for the ML estimate.

Table 4.3: Probability of selecting the right copula function.

(Measurements, Units)	Method	NRE	REB
(25,3)	Bay	0.82	0.99
	BayF	0.84	0.99
	ML	0.36	0.79
(50,3)	Bay	0.90	1.00
	BayF	0.88	1.00
	ML	0.25	1.00
(25,6)	Bay	0.82	1.00
	BayF	0.81	1.00
	ML	0.31	0.87

Figure 4.9 presents the average percentage error on the estimate of the copula parameter when the correct copula was identified. Both methods tend to severely underestimate the value of the copula parameter. This suggests that the MTTF and reliability estimates would be biased even if the true parameters of the degradation processes were known and only the copula parameter were estimated.

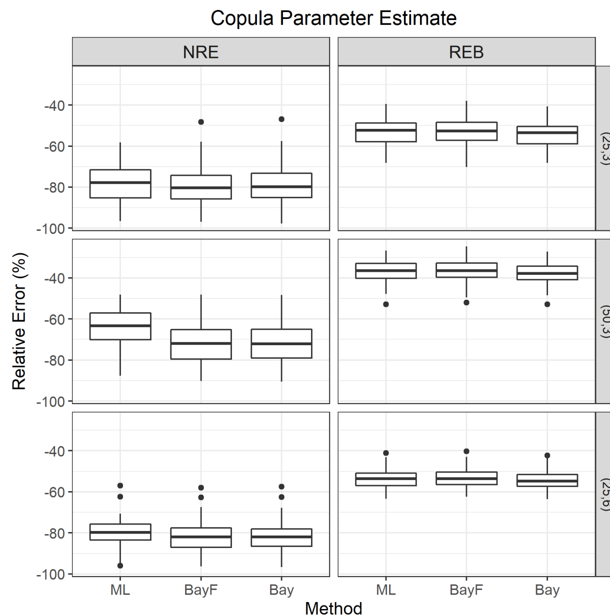

Figure 4.9: Relative error of the copula parameter estimate.

4.5 Conclusions

In this paper, we proposed the first parametric model to analyze accelerated reliability growth data based on multiple correlated degradation processes. The dependency between degradation increments is modeled using a copula function. The model addresses random effects by assigning a probability distribution on the base-line inverse-mean and the diffusion parameters and incorporates explanatory variables that change the inverse-mean parameter. We developed Bayesian and ML methods to estimate the model parameters using a two-stage process, and the copula function was selected based on the BIC or EBIC score among multiple choices.

We presented numerical examples to illustrate the effectiveness of the proposed methods to

capture the final reliability function of a system. In particular, the ML methods are better at identifying the absence of random effects. On the other hand, the Bayesian methods with informative priors are better at estimating the general location of the system's reliability function and MTTF. Moreover, both methods show similar performance as the amount of data increases due to increasing the number of measurements taken from each unit or the number of units tested. These results illustrate the usefulness of Bayesian models at early development stages when the testing data is scarce for selecting the correct copula function and predicting the MTTF. On the other hand, the extra computational time required to sample the posterior distribution loses its advantage as more data becomes available. Finally, this model could be used to support resource allocation decisions like whether to test a small number of units for a long period of time or a large number of units for a short time period.

There are several directions for future research. First, it is worth investigating efficient ways to improve the accuracy of the estimates of the parameters of the copula function. Moreover, different versions of degradation models need to be developed for non-monotonic degradation processes. In addition, more efficient methods to model high-dimensional correlated degradation processes will be investigated in our future work. Lastly, there are no efficient methods to estimate the credible intervals (Bayesian) for the system reliability and MTTF. This is due to the two-step estimation procedure which does not provide samples of all the model parameters. On the other hand, the confidence intervals (ML) for this quantities can be obtained using a parametric Bootstrap procedure (Nikoloulopoulos & Karlis, 2008), although with a relatively high computational cost..

References

Banerjee, A. K. & Bhattacharyya, G. K. (1979). Bayesian results for the Inverse Gaussian distribution with an application. *Technometrics*, *21*(2), 247–251.

Chen, S. X. & Huang, T.-M. (2007). Nonparametric estimation of copula functions for dependence modelling. *Canadian Journal of Statistics*, *35*(2), 265–282.

Crow, L. H. (2004). An extended reliability growth model for managing and assessing corrective actions. In *2004 Proceedings Annual Reliability and Maintainability Symposium - RAMS*, (pp. 73–80).

dos Santos Silva, R. & Lopes, H. (2008). Copula, marginal distributions and model selection: A bayesian note. *Statistics and Computing*, *18*, 313–320.

Gabraeel, N. Z., Lawley, M. A., Li, R., & Ryan, J. K. (2005). Residual-life distributions from component degradation signals: A Bayesian approach. *IIE Transactions*, *37*(6), 543–557.

Hamada, M. (2005). Using degradation data to assess reliability. *Quality Engineering*, *17*(4), 615–620.

Hamada, M. S., Wilson, A. G., Reese, C. S., & Martz, H. F. (2008). *Bayesian reliability* (1 ed.). Springer New York.

Hong, Y., Zhang, M., & Meeker, W. (2018). Big data and reliability applications: The complexity dimension. *Journal of Quality Technology*, *50*.

Huard, D., Évin, G., & Favre, A.-C. (2006). Bayesian copula selection. *Computational Statistics & Data Analysis*, *51*(2), 809 – 822.

Lawless, J. & Crowder, M. (2004). Covariates and random effects in a Gamma process model with application to degradation and failure. *Lifetime Data Analysis*, *10*(3), 213–227.

Liao, H. & Elsayed, E. A. (2006). Reliability inference for field conditions from accelerated degradation testing. *Naval Research Logistics (NRL)*, *53*(6), 576–587.

Lu, D., Pandey, M. D., & Xie, W.-C. (2013). An efficient method for the estimation of parameters of stochastic gamma process from noisy degradation measurements. *Proceedings of the Institution of Mechanical Engineers*, *227*(4), 425.

Martz, H. & Waller, R. (1991). *Bayesian reliability analysis* (1 ed.). Krieger Publishing Company.

Nelson, W. (1990). *Accelerated testing - statistical models, test plans, and data analysis*. John Wiley & Sons, Hoboken, New Jersey.

Nikoloulopoulos, A. K. & Karlis, D. (2008). Copula model evaluation based on parametric bootstrap. *Computational Statistics & Data Analysis*, *52*(7), 3342 – 3353.

Park, S.-H. & Kim, J.-H. (2017). Application of gamma process model to estimate the lifetime of photovoltaic modules. *Solar Energy*, *147*, 390 – 398.

Peng, C.-Y. (2015). Inverse Gaussian processes with random effects and explanatory variables for degradation data. *Technometrics*, *57*(1), 100–111.

Peng, W., Li, Y., Yang, Y., Zhu, S., & Huang, H. (2016). Bivariate analysis of incomplete degradation observations based on inverse gaussian processes and copulas. *IEEE Transactions on Reliability*, *65*(2), 624–639.

Ruiz, C., Heydari, M., Sullivan, K. M., Liao, H., & Pohl, E. (2020). Data analysis and resource al-

location in bayesian selective accelerated reliability growth. *IISE Transactions*, *52*(3), 301–320.

Ruiz, C., Liao, H., & Pohl, E. (2019). A nonparametric degradation-based method for modeling reliability growth. In *2019 Annual Reliability and Maintainability Symposium (RAMS)*, (pp. 1–6).

Ruiz, C., Pohl, E., Liao, H., & Sullivan, K. M. (2019). A bayesian framework for accelerated reliability growth testing with multiple sources of uncertainty. *Quality and Reliability Engineering International*, *35*(3), 837–853.

Schepsmeier, U., Stoeber, J., Brechmann, E. C., Graeler, B., Nagler, T., & Erhardt, T. (2018). *VineCopula: Statistical Inference of Vine Copulas*. R package version 2.1.8.

Strunz, R. & Herrmann, J. W. (2012). Planning, tracking, and projecting reliability growth a Bayesian approach. In *2012 Proceedings Annual Reliability and Maintainability Symposium - RAMS*, (pp. 1–6).

Sun, Q., Ye, Z.-S., & Hong, Y. (2019). Statistical modeling of multivariate destructive degradation tests with blocking. *Technometrics*, *0*(0), 1–13.

Wang, X. (2010). Wiener processes with random effects for degradation data. *Journal of Multivariate Analysis*, *101*(2), 340–351.

Wang, X., Balakrishnan, N., Guo, B., & Jiang, P. (2015). Residual life estimation based on bivariate non-stationary gamma degradation process. *Journal of Statistical Computation and Simulation*, *85*(2), 405.

Wayne, M. & Modarres, M. (2015). A Bayesian model for complex system reliability growth under arbitrary corrective actions. *IEEE Transactions on Reliability*, *64*(1), 206–220.

Wilson, A. G. & Fronczyk, K. M. (2017). Bayesian reliability: Combining information. *Quality Engineering*, *29*(1), 119–129.

Ye, Z.-S. & Chen, N. (2014). The Inverse Gaussian process as a degradation model. *Technometrics*, *56*(3), 302–311.

Ye, Z.-S., Xie, M., Tang, L.-C., & Chen, N. (2014). Semiparametric estimation of gamma processes for deteriorating products. *Technometrics*, *56*(4), 504–513.

Appendix: Some Derivations

PDF of the degradation increments under the REM model.

The PDF of degradation increments of unit k after n_k measurements is:

$$\begin{aligned} f(\Delta\mathbf{y}_{ik}) &= \int_0^\infty \prod_{j=1}^{n_k} \left[\sqrt{\frac{\lambda_i \Delta h_{ijk}^2}{2\pi \Delta y_{ijk}^3}}\right] \exp\left(\sum_{j=1}^{n_k} \frac{-\lambda_i m_i^2}{2\Delta y_{ijk}} \left[\Delta y_{ijk} - \frac{\Delta h_{ijk}}{m_i}\right]^2\right) \\ &\quad \times \frac{\sqrt{\tau_i}}{\sqrt{2\pi}} \exp\left(-\frac{\tau_i}{2}(m_{0i} - \nu_i)^2\right) \frac{1}{\Phi'\left(-\nu_i\sqrt{\tau_i}\right)} dm_{0i} \\ &= \frac{1}{\Phi'\left(-\nu_i\sqrt{\tau_i}\right)} \prod_{j=1}^{n_k} \sqrt{\frac{\lambda_i \Delta h_{ijk}^2}{2\pi \Delta y_{ijk}^3}} \\ &\quad \times \int_0^\infty \frac{\sqrt{\tau_i}}{\sqrt{2\pi}} \exp\left(\sum_{j=1}^{n_k} \frac{-\lambda_i m_i^2}{2\Delta y_{ijk}} \left[\Delta y_{ijk} - \frac{\Delta h_{ijk}}{m_i}\right]^2 - \frac{\tau_i}{2}\left(m_{0i} - \nu_i\right)^2\right) dm_{0i}. \end{aligned}$$

where $m_i = \mu_i^{-1}$. In order to evaluate this expression, we first let:

$$\gamma = -\frac{\lambda_i}{2} \sum_{j=1}^{n_k} \left[\Delta y_{ijk} m_i^2 - 2m_i \Delta h_{ijk} + \frac{\Delta h_{ijk}^2}{\Delta y_i jk}\right] - \frac{\tau_i}{2}(m_{0i}^2 - 2\nu_i m_{0i} + \nu_i^2).$$

Then, we have:

$$\begin{aligned} \gamma &= -\frac{\lambda_i}{2} Y_{ik} m_{0i}^2 \mu_{xik}^2 - \frac{\tau_i}{2} m_{0i}^2 + \frac{\lambda_i}{2} 2m_{0i}\mu_{xik} H_{ik} + \frac{\tau_i}{2} 2\nu_i m_{0i} - \frac{\lambda_i}{2} HY_{ik} - \frac{\tau_i}{2}\nu_i^2 \\ &= -\frac{1}{2}\left[m_{0i}^2(\lambda_i Y_{ik}\mu_{xik}^2 + \tau_i) - 2m_{0i}(\lambda_i \mu_{xik} H_{ik} + \nu_i\tau_i)\right] - \frac{1}{2}\left[\lambda_i HY_{ik} + \tau_i\nu_i^2\right] \\ &= -\frac{\lambda_i Y_{ik}\mu_{xik}^2 + \tau_i}{2}\left[m_{0i}^2 - 2m_{0i}\frac{\lambda_i \mu_{xik} H_{ik} + \nu_i\tau_i}{\lambda_i Y_{ik}\mu_{xik}^2 + \tau_i}\right] - \frac{1}{2}\left[\lambda_i HY_{ik} + \tau_i\nu_i^2\right] \\ &= -\frac{\lambda_i Y_{ik}\mu_{xik}^2 + \tau_i}{2}\left[m_{0i} - \frac{\lambda_i \mu_{xik} H_{ik} + \nu_i\tau_i}{\lambda_i Y_{ik}\mu_{xik}^2 + \tau_i}\right]^2 - \frac{1}{2}\left[\lambda_i HY_{ik} + \tau_i\nu_i^2 - \frac{(\lambda_i \mu_{xik} H_{ik} + \nu_i\tau_i)^2}{\lambda_i Y_{ik}\mu_{xik}^2 + \tau_i}\right] \\ &= -\frac{\gamma_1}{2} - \frac{\gamma_2}{2}, \end{aligned}$$

where γ_1 and γ_2 are defined as:

$$\gamma_1 = \left(\lambda_i Y_{ik}\mu_{xik}^2 + \tau_i\right)\left[m_{0i} - \frac{\lambda_i \mu_{xik} H_{ik} + \nu_i\tau_i}{\lambda_i Y_{ik}\mu_{xik}^2 + \tau_i}\right]^2,$$

$$\gamma_2 = \left[\lambda_i HY_{ik} + \tau_i \nu_i^2 - \frac{(\lambda_i \mu_{xik} H_{ik} + \nu_i \tau_i)^2}{\lambda_i Y_{ik} \mu_{xik}^2 + \tau_i} \right].$$

As a result, the PDF of degradation increments $f(\Delta \mathbf{y}_{ik})$ can be rewritten as:

$$\begin{aligned} f(\Delta \mathbf{y}_{ik}) &= \frac{1}{\Phi'(-\nu_i \sqrt{\tau_i})} \prod_{j=1}^{n_k} \sqrt{\frac{\lambda_i \Delta h_{ijk}^2}{2\pi \Delta y_{ijk}^3}} \sqrt{\frac{\tau_i}{\lambda_i Y_{ik} \mu_{xik}^2 + \tau_i}} \exp\left(-\frac{\gamma_2}{2}\right) \\ &\times \int_0^\infty \sqrt{\frac{\lambda_i Y_{ik} \mu_{xik}^2 + \tau_i}{2\pi}} \exp\left(-\frac{\gamma_1}{2}\right) dm_{0i} \\ &= \frac{1}{\Phi'(-\nu_i \sqrt{\tau_i})} \prod_{j=1}^{n_k} \sqrt{\frac{\lambda_i \Delta h_{ijk}^2}{2\pi \Delta y_{ijk}^3}} \sqrt{\frac{\tau_i}{\lambda_i Y_{ik} \mu_{xik}^2 + \tau_i}} \exp\left(\frac{-\gamma_2}{2}\right) \Phi' \left(\frac{-\lambda_i \mu_{xik} H_{ik} - \nu_i \tau_i}{\sqrt{\lambda_i Y_{ik} \mu_{xik}^2 + \tau_i}} \right). \end{aligned}$$

PDF of the degradation increments under the REB model.

Similarly to the REM model,

$$\begin{aligned} f(\Delta \mathbf{y}_{ik}) &= \int_0^\infty \int_0^\infty \prod_{j=1}^{n_k} \left[\sqrt{\frac{\lambda_i \Delta h_{ijk}^2}{2\pi \Delta y_{ijk}^3}} \right] \exp\left(\sum_{j=1}^{n_k} \frac{-\lambda_i m_i^2}{2\Delta y_{ijk}} \left[\Delta y_{ijk} - \frac{\Delta h_{ijk}}{m_i} \right]^2 \right) \\ &\times \frac{\beta_i^{\alpha_i}}{\Gamma(\alpha_i)} \lambda_i^{\alpha_i - 1} \exp(-\beta_i \lambda_i) \sqrt{\frac{\lambda_i \tau_i}{2\pi}} \exp\left(-\frac{\lambda_i \tau_i (m_i - \nu_i)^2}{2} \right) \frac{1}{\Upsilon'_{2\alpha_i}(-\nu_i \sqrt{\tau_i \alpha_i / \beta_i})} d\lambda_i dm_{0i}. \end{aligned}$$

By only considering the terms related to λ_i, the inner integral can be obtained as:

$$\begin{aligned} I_\lambda &= \int_0^\infty \lambda_i^{n_k/2} \exp\left(\sum_{j=1}^{n_k} \frac{-\lambda_i m_i^2}{2\Delta y_{ijk}} \left[\Delta y_{ijk} - \frac{\Delta h_{ijk}}{m_i} \right]^2 \right) \lambda_i^{\alpha_i - 1/2} \exp\left(-\lambda_i \left[\beta_i + \frac{\tau_i (m_i - \nu_i)^2}{2} \right] \right) d\lambda_i \\ &= \int_0^\infty \lambda_i^{\alpha_i + (n_k+1)/2 - 1} \exp\left(-\lambda_i \left[\beta_i + \frac{\tau_i (m_i - \nu_i)^2}{2} + \sum_{j=1}^{n_k} \frac{m_i^2}{2\Delta y_{ijk}} \left[\Delta y_{ijk} - \frac{\Delta h_{ijk}}{m_i} \right]^2 \right] \right) d\lambda_i. \end{aligned}$$

By defining the auxiliary variable γ as:

$$\gamma = \beta_i + \frac{\tau_i (m_i - \nu_i)^2}{2} + \sum_{j=1}^{n_k} \frac{m_i^2}{2\Delta y_{ijk}} \left[\Delta y_{ijk} - \frac{\Delta h_{ijk}}{m_i} \right]^2,$$

the integral becomes:

$$I_\lambda = \int_0^\infty \lambda_i^{\alpha_i+(n_k+1)/2-1} \exp\left(-\lambda_i \gamma\right) d\lambda_i = \frac{\Gamma(\alpha_i + (n_k+1)/2)}{\gamma^{\alpha_i+(n_k+1)/2}}.$$

Then, by integrating with respect to m_{0i}, we have:

$$f(\Delta \mathbf{y}_{ik}) = \prod_{j=1}^{n_k} \left[\sqrt{\frac{\Delta h_{ijk}^2}{2\pi \Delta y_{ijk}^3}} \right] \frac{1}{\Upsilon'_{2\alpha_i}(-\nu_i \sqrt{\tau_i \alpha_i/\beta_i})} \frac{\beta_i^{\alpha_i}}{\Gamma(\alpha_i)} \sqrt{\frac{\tau_i}{2}} \int_0^\infty \sqrt{\frac{1}{\pi}} \frac{\Gamma(\alpha_i + (n_k+1)/2)}{\gamma^{\alpha_i+(n_k+1)/2}} dm_{0i}.$$

The integrand can be re-expressed as the PDF of the Student's t-distribution times a constant by noting that:

$$\begin{aligned}
\gamma &= \beta_i + \frac{1}{2}\left[HY_{ik} + \tau_i \nu_i^2 - \frac{(\mu_{xik} H_{ik} + \nu_i \tau_i)^2}{Y_{ik}\mu_{xik}^2 + \tau_i}\right] + \frac{Y_{ik}\mu_{xik}^2 + \tau_i}{2}\left[m_{0i} - \frac{\mu_{xik} H_{ik} + \nu_i \tau_i}{Y_{ik}\mu_{xik}^2 + \tau_i}\right]^2 \\
&= \gamma_1 + \frac{\gamma_2}{2}(m_{0i} - \nu')^2,
\end{aligned}$$

where

$$\gamma_1 = \beta_i + \frac{1}{2}\left[HY_{ik} + \tau_i \nu_i^2 - \frac{(\mu_{xik} H_{ik} + \nu_i \tau_i)^2}{Y_{ik}\mu_{xik}^2 + \tau_i}\right], \quad \gamma_2 = Y_{ik}\mu_{xik}^2 + \tau_i, \quad \nu' = \frac{\mu_{xik} H_{ik} + \nu_i \tau_i}{Y_{ik}\mu_{xik}^2 + \tau_i}.$$

By replacing γ in the integral, we get:

$$\begin{aligned}
I_m &= \int_0^\infty \sqrt{\frac{1}{\pi}} \Gamma(\alpha_i + (n_{ik}+1)/2) \left[\gamma_1 + \frac{\gamma_2}{2}(m_{0i} - \nu')^2\right]^{-\alpha_i-(n_k+1)/2} dm_{0i} \\
&= \int_0^\infty \frac{\Gamma(\alpha_i + (n_k+1)/2)}{\sqrt{\pi}\gamma_1^{\alpha_i+(n_k+1)/2}} \left[1 + \frac{\gamma_2}{2\gamma_1}(m_{0i} - \nu')^2\right]^{-\alpha_i-(n_k+1)/2} dm_{0i} \\
&= \frac{\Gamma(\alpha_i + n_k/2)}{\gamma_1^{\alpha_i+(n_k+1)/2}} \sqrt{\frac{2\gamma_1}{\gamma_2}} \int_0^\infty \frac{\Gamma(\alpha_i + (n_k+1)/2)}{\Gamma(\alpha_i + n_k/2)\sqrt{\pi}} \\
&\times \sqrt{\frac{\gamma_2(2\alpha_i + n_k)}{2\gamma_1(2\alpha_i + n_k)}} \left[1 + \frac{\gamma_2(2\alpha_i + n_k)}{2\gamma_1(2\alpha_i + n_k)}(m_{0i} - \nu')^2\right]^{-\alpha_i-(n_k+1)/2} dm_{0i} \\
&= \frac{\Gamma(\alpha_i + (n_k)/2)}{\gamma_1^{\alpha_i+n_k/2}} \sqrt{\frac{2}{\gamma_2}} \Upsilon'_{2\alpha_i+n_k}\left(-\nu' \sqrt{\frac{\gamma_2(2\alpha_i + n_k)}{2\gamma_1}}\right).
\end{aligned}$$

Then, the PDF of degradation increments under the REB model can be expressed as:

$$
\begin{aligned}
f(\Delta \mathbf{y}_{ik}) = &\prod_{j=1}^{n_k} \left[\sqrt{\frac{\Delta h_{ijk}^2}{2\pi \Delta y_{ijk}^3}} \right] \frac{1}{\Upsilon'_{2\alpha_i}(-\nu_i \sqrt{\tau_i \alpha_i / \beta_i})} \frac{\beta_i^{\alpha_i}}{\Gamma(\alpha_i)} \sqrt{\frac{\tau_i}{Y_{ik}\mu_{xik}^2 + \tau_i}} \frac{\Gamma(\alpha_i + n_k/2)}{\omega_{ik}^{\alpha_i + n_k/2}} \\
&\times \Upsilon'_{2\alpha_i + n_k} \left(-\left[\mu_{xik} H_{ik} + \nu_i \tau_i\right] \sqrt{\frac{2\alpha_i + n_k}{2(Y_{ik}\mu_{xik}^2 + \tau_i)\omega_{ik}}} \right),
\end{aligned}
\tag{4.19}
$$

where

$$
\omega_{ik} = \beta_i + \frac{1}{2} \left[HY_{ik} + \tau_i \nu_i^2 - \frac{(\mu_{xik} H_{ik} + \nu_i \tau_i)^2}{Y_{ik}\mu_{xik}^2 + \tau_i} \right].
$$

5 Summary

Reliability growth programs are important tools to ensure that newly designed products or system achieve a minimum reliability requirement in a short development time. Reliability growth programs consists of a series of stages the system design is changed to improve its reliability. Due to cost and time constraints, reliability analysis of complex multi-component systems is based on accelerated testing at component and subsystem level. However, reliability growth models in the literature only consider single component systems or series systems and often struggle to accurately incorporate accelerated test data in the analysis. In this dissertation, we develop new methodologies for analyzing time-to-failure data and we propose the first methodologies for analyzing degradation data in the context of a multi-stage reliability growth program with testing at component level.

For analyzing time-to-failure data, we develop a Bayesian reliability growth framework to predict component reliability, and propose a procedure to aggregate component results to predict the reliability of the system. A numerical example with simulated data illustrates the superior performance of the proposed method when compared to widely used reliability growth methodologies. In this dissertation, we propose the first models for modeling reliability growth based on degradation data. We propose a non-parametric model for the case when components only fail due to a single degradation process. In addition, we develop a novel degradation-based reliability growth model for a component with multiple correlated degradation processes. Numerical examples using simulated data are presented to validate the accuracy of the proposed methodologies.

This dissertation has the potential to change the way reliability growth is performed by developing methodologies for statistical analysis of degradation data which can be combined with existing physics-of-failure approaches. There are still multiple open research directions such as the development of more efficient statistical models to analyze high-dimensional degradation data, characterization of reliability growth with both time-to-failure and degradation data, and the development of statistical tests to assess the introduction or removal of random effects after design changes.